

Supplementary Materials

Tri-*tert*-butyl(*n*-alkyl)phosphonium ionic liquids: structure, properties and application as hybrid catalyst nanomaterials

by Daria M. Arkhipova, Vadim V. Ermolaev, Vasily A. Miluykov, Farida G. Valeeva, Gulnara A. Gaynanova, Lucia Ya. Zakharova, Mikhail E. Minyaev and Valentin P. Ananikov

The synthetic procedures of the PILs

Tri-*tert*-butyl(methyl)phosphonium iodide (1a)

0.6 mL (10.3 mmol) iodomethane was added to 2.1 g (10.3 mmol) tri-*tert*-butylphosphine at -70°C. The mixture was allowed to reach room temperature. Formed white solid was washed with diethyl ether (3 X 10 mL); the residue of solvent was removed *in vacuo*.

White crystalline solid: 3.5 g, 99%; decomp. 297.0 °C; ¹H NMR (CDCl₃, 300.13 MHz) δ 2.11 (d, ²J_{PH} = 11.42 Hz, 3H, P-CH₃), 1.64 (d, ³J_{PH} = 14.32 Hz, 27H, P(C(CH₃)₃)₃). ¹³C NMR (CDCl₃, 75.47 MHz) δ 38.1 (d, ¹J_{PC} = 31.7 Hz, P(C(CH₃)₃)₃), 29.6 (s, P(C(CH₃)₃)₃), 3.1 (d, ¹J_{PC} = 42.5 Hz, P-CH₃). ³¹P NMR (CDCl₃, 121.54 MHz) δ 51.3 (s). *m/z*: 217.2094 (C₁₃H₃₀P⁺, 100%).

Tri-*tert*-butyl(methyl)phosphonium tetrafluoroborate (1b)

0.6 g (5.1 mmol) NaBF₄ was added to the solution of 1.2 g (3.4 mmol) tri-*tert*-butyl(methyl)phosphonium iodide in 9 mL H₂O. White precipitate was formed, it was filtered, dissolved in CH₂Cl₂ and dried over MgSO₄ overnight. Then solution was filtered and dried *in vacuo*.

White crystalline solid: 0.5 g, 41%; decomp. 315.0 °C; ¹H NMR (CDCl₃, 300.13 MHz) δ 1.90 (d, ²J_{PH} = 11.59 Hz, 3H, P-CH₃), 1.62 (d, ³J_{PH} = 14.06 Hz, 27H, P(C(CH₃)₃)₃). ¹³C NMR (CDCl₃, 75.47 MHz) δ 37.9 (d, ¹J_{PC} = 32.1 Hz, P(C(CH₃)₃)₃), 29.1 (s, P(C(CH₃)₃)₃), 0.4 (d, ¹J_{PC} = 45.8 Hz, P-CH₃). ³¹P NMR (CDCl₃, 121.54 MHz) δ 51.0 (s). *m/z*: 217.2083 (C₁₃H₃₀P⁺, 100%).

Tri-*tert*-butyl(propyl)phosphonium iodide (2a)

The mixture of 3.1 g (15.3 mmol) tri-*tert*-butylphosphine and 1.5 mL (15.3 mmol) 1-iodopropane was stirred for 3 hours at room temperature. The reaction mixture was washed with diethyl ether (3 X 20 mL) and dried *in vacuo*.

White powder: 4.1 g, 71%; mp. 154.0 °C; ¹H NMR (CDCl₃, 300.13 MHz) δ 2.60 (m, 2H, P-CH₂), 2.03 (m, 2H, P-CH₂-CH₂), 1.70 (d, ³J_{PH} = 14.09 Hz, 27H, P(C(CH₃)₃)₃), 1.34 (t, ³J_{HH} = 7.16 Hz, ³J_{PH} = 2.50 Hz, 3H, CH₂-CH₃). ¹³C NMR (CDCl₃, 75.47 MHz) δ 39.4 (d, ¹J_{PC} = 29.3 Hz, P(C(CH₃)₃)₃), 30.2 (s, P(C(CH₃)₃)₃), 21.0 (d, ¹J_{PC} = 34.6 Hz, P-CH₂), 19.0 (d, ²J_{PC} = 6.3 Hz, P-CH₂-CH₂), 16.9 (d, ³J_{PC} = 13.8 Hz, CH₂-CH₃). ³¹P NMR (CDCl₃, 121.54 MHz) δ 50.7 (s). *m/z*: 245.2390 (C₁₅H₃₄P⁺, 100%).

Tri-*tert*-butyl(propyl)phosphonium tetrafluoroborate (2b)

1.4 g (12.5 mmol) NaBF₄ was added to the solution of 3.1 g (8.3 mmol) tri-*tert*-butyl(propyl)phosphonium iodide in 15 mL H₂O. White precipitate was formed, it was filtered, dissolved in CH₂Cl₂ and dried over MgSO₄ overnight. Then solution was filtered and dried *in vacuo*.

White powder: 2.0 g, 73%; mp. 222.0 °C; ¹H NMR (CDCl₃, 300.13 MHz) δ 2.33 (m, 2H, P-CH₂), 1.98 (m, 2H, P-CH₂-CH₂), 1.64 (d, ³J_{PH} = 14.00 Hz, 27H, P(C(CH₃)₃)₃), 1.23 (t, ³J_{HH} = 7.19 Hz, ³J_{PH} = 2.43 Hz, 3H, CH₂-CH₃). ¹³C NMR (CDCl₃, 75.47 MHz) δ 39.2 (d, ¹J_{PC} = 29.4 Hz, P(C(CH₃)₃)₃), 29.8 (s, P(C(CH₃)₃)₃), 20.4 (d, ¹J_{PC} = 35.2 Hz, P-CH₂), 18.9 (d, ²J_{PC} = 6.4 Hz, P-CH₂-CH₂), 16.3 (d, ³J_{PC} = 14.2 Hz, CH₂-CH₃). ³¹P NMR (CDCl₃, 121.54 MHz) δ 49.2 (s). *m/z*: 245.2390 (C₁₅H₃₄P⁺, 100%).

Tri-*tert*-butyl(pentyl)phosphonium bromide (3a)

The mixture of 2.0 g (9.7 mmol) tri-*tert*-butylphosphine and 1.2 mL (9.7 mmol) 1-bromopentane was stirred for 6 hours at 100°C. After cooling the reaction mixture was washed with diethyl ether (3 X 10 mL) and dried *in vacuo*.

White powder: 2.9 g, 83%; mp. 172.8°C; ¹H NMR (CDCl₃, 300.13 MHz) δ 2.54 (m, 2H, P-CH₂), 1.90 (m, 2H, P-CH₂-CH₂), 1.65 (d, ³J_{PH} = 13.93 Hz, 27H, P(C(CH₃)₃)₃), 1.63 (m, 2H, P-CH₂-CH₂-CH₂), 1.36 (m, 2H,

$CH_2\text{-}CH_3$), 0.90 (t, $^3J_{HH}$ = 7.32 Hz, 3H, $CH_2\text{-}CH_3$). ^{13}C NMR ($CDCl_3$, 75.47 MHz) δ 39.4 (d, $^1J_{PC}$ = 29.2 Hz, $P(C(CH_3)_3)_3$), 33.8 (d, $^3J_{PC}$ = 12.4 Hz, P- $CH_2\text{-}CH_2\text{-}CH_2$), 30.1 (s, $P(C(CH_3)_3)_3$), 24.9 (d, $^2J_{PC}$ = 6.6 Hz, P- $CH_2\text{-}CH_2$), 22.3 (s, $CH_2\text{-}CH_3$), 19.0 (d, $^1J_{PC}$ = 34.3 Hz, P- CH_2), 13.8 (c, $CH_2\text{-}CH_3$). ^{31}P NMR ($CDCl_3$, 121.54 MHz) δ 48.8 (s). *m/z*: 273.2706 ($C_{17}H_{38}P^+$, 100%).

Tri-*tert*-butyl(pentyl)phosphonium tetrafluoroborate (3b)

1.2 g (11.3 mmol) $NaBF_4$ was added to the solution of 2.0 g (5.7 mmol) tri-*tert*-butyl(pentyl)phosphonium bromide in 10 mL H_2O . White precipitate was formed, it was filtered, dissolved in CH_2Cl_2 and dried over $MgSO_4$ overnight. Then solution was filtered and dried *in vacuo*.

White powder: 1.7 g, 83%; mp. 190.0 °C; 1H NMR ($CDCl_3$, 300.13 MHz) δ 2.32 (m, 2H, P- CH_2), 1.92 (m, 2H, P- $CH_2\text{-}CH_2$), 1.66 (d, $^3J_{PH}$ = 14.03 Hz, 27H, $P(C(CH_3)_3)_3$), 1.59 (m, 2H, P- $CH_2\text{-}CH_2\text{-}CH_2$), 1.41 (m, 2H, $CH_2\text{-}CH_3$), 0.95 (t, $^3J_{HH}$ = 7.23 Hz, 3H, $CH_2\text{-}CH_3$). ^{13}C NMR ($CDCl_3$, 75.47 MHz) δ 39.3 (d, $^1J_{PC}$ = 29.1 Hz, $P(C(CH_3)_3)_3$), 33.7 (d, $^3J_{PC}$ = 12.6 Hz, P- $CH_2\text{-}CH_2\text{-}CH_2$), 29.8 (s, $P(C(CH_3)_3)_3$), 24.7 (d, $^2J_{PC}$ = 6.7 Hz, P- $CH_2\text{-}CH_2$), 22.2 (s, $CH_2\text{-}CH_3$), 18.5 (d, $^1J_{PC}$ = 35.3 Hz, P- CH_2), 13.8 (s, $CH_2\text{-}CH_3$). ^{31}P NMR ($CDCl_3$, 121.54 MHz) δ 49.2 (s). *m/z*: 273.2718 ($C_{17}H_{38}P^+$, 100%).

Tri-*tert*-butyl(heptyl)phosphonium bromide (4a)

The mixture of 2.5 g (12.1 mmol) tri-*tert*-butylphosphine and 1.9 mL (12.1 mmol) 1-bromoheptane was stirred for 5 hours at 100°C. The reaction mixture was washed with diethyl ether (3 X 10 mL) and dried *in vacuo*.

White powder: 2.1 g, 45%; 124.9 °C. 1H NMR ($CDCl_3$, 300.13 MHz) δ 2.56 (m, 2H, P- CH_2), 1.91 (m, 2H, P- $CH_2\text{-}CH_2$), 1.67 (d, $^3J_{PH}$ = 13.77 Hz, 27H, $P(C(CH_3)_3)_3$), 1.67 (m, 2H, P- $CH_2\text{-}CH_2\text{-}CH_2$), 1.38-1.25 (m, 6H, CH_2), 0.87 (t, $^3J_{HH}$ = 6.84 Hz, 3H, $CH_2\text{-}CH_3$). ^{13}C NMR ($CDCl_3$, 75.47 MHz) δ 39.3 (d, $^1J_{PC}$ = 29.4 Hz, $P(C(CH_3)_3)_3$), 31.8 (d, $^3J_{PC}$ = 12.5 Hz, P- $CH_2\text{-}CH_2\text{-}CH_2$), 31.4 (s, CH_2), 30.1 (s, $P(C(CH_3)_3)_3$), 28.8 (s, CH_2), 25.2 (d, $^2J_{PC}$ = 6.5 Hz, P- $CH_2\text{-}CH_2$), 22.5 (s, CH_2), 19.1 (d, $^1J_{PC}$ = 34.7 Hz, P- CH_2), 13.9 (s, $CH_2\text{-}CH_3$). ^{31}P NMR ($CDCl_3$, 121.54 MHz) δ 49.4 (s). *m/z*: 301.3019 ($C_{19}H_{42}P^+$, 100%).

Tri-*tert*-butyl(heptyl)phosphonium tetrafluoroborate (4b)

0.8 g (7.3 mmol) $NaBF_4$ was added to 1.4 g (3.7 mmol) tri-*tert*-butyl(octyl)phosphonium bromide dissolved in 11 mL H_2O . White precipitate was formed, filtered, dissolved in CH_2Cl_2 and dried over $MgSO_4$ overnight. Then solution was filtered and dried *in vacuo*.

White powder: 1.3 g, 88%; mp. 123.0 °C. 1H NMR ($CDCl_3$, 300.13 MHz) δ 2.29 (m, 2H, P- CH_2), 1.90 (m, 2H, P- $CH_2\text{-}CH_2$), 1.65 (d, $^3J_{PH}$ = 14.00 Hz, 27H, $P(C(CH_3)_3)_3$), 1.57 (m, 2H, P- $CH_2\text{-}CH_2\text{-}CH_2$), 1.32 (m, 6H, CH_2), 0.89 (t, $^3J_{HH}$ = 6.50 Hz, 3H, $CH_2\text{-}CH_3$). ^{13}C NMR ($CDCl_3$, 75.47 MHz) δ 39.3 (d, $^1J_{PC}$ = 29.2 Hz, $P(C(CH_3)_3)_3$), 31.7 (d, $^3J_{PC}$ = 12.7 Hz, P- $CH_2\text{-}CH_2\text{-}CH_2$), 31.5 (s, CH_2), 29.8 (s, $P(C(CH_3)_3)_3$), 28.8 (s, CH_2), 25.1 (d, $^2J_{PC}$ = 6.6 Hz, P- $CH_2\text{-}CH_2$), 22.6 (s, CH_2), 18.5 (d, $^1J_{PC}$ = 35.2 Hz, P- CH_2), 14.0 (s, $CH_2\text{-}CH_3$). ^{31}P NMR ($CDCl_3$, 121.54 MHz) δ 47.7 (s). *m/z*: 301.3017 ($C_{19}H_{42}P^+$, 100%).

Tri-*tert*-butyl(nonyl)phosphonium bromide (5a)

The mixture of 2.5 g (12.4 mmol) tri-*tert*-butylphosphine and 2.4 mL (12.4 mmol) 1-bromononane was stirred for 5 hours at 100°C. The reaction mixture was washed with diethyl ether (3 X 15 mL) and dried *in vacuo*.

White powder: 3.2 g, 63%; mp. 116.4 °C; 1H NMR ($CDCl_3$, 300.13 MHz) δ 2.49 (m, 2H, P- CH_2), 1.86 (m, 2H, P- $CH_2\text{-}CH_2$), 1.63 (d, $^3J_{PH}$ = 13.81 Hz, 27H, $P(C(CH_3)_3)_3$), 1.63 (m, 2H), 1.32-1.18 (m, 12H), 0.82 (t, $^3J_{HH}$ = 7.16 Hz, 3H, $CH_2\text{-}CH_3$). ^{13}C NMR ($CDCl_3$, 75.47 MHz) δ = 39.4 (d, $^1J_{PC}$ = 29.2 Hz, $C(CH_3)_3$), 31.8 (d, $^3J_{PC}$ = 12.4 Hz, P- $CH_2\text{-}CH_2\text{-}CH_2$), 31.7 (s, CH_2), 30.1 (s, $C(CH_3)_3$), 29.2 (s, CH_2), 29.1 (s, CH_2), 25.2 (d, $^2J_{PH}$ = 6.6 Hz, P- $CH_2\text{-}CH_2$), 22.5 (s, $CH_2\text{-}CH_3$), 19.1 (d, $^1J_{PC}$ = 34.6 Hz, P- CH_2), 14.0 (s, $CH_2\text{-}CH_3$). ^{31}P NMR ($CDCl_3$, 121.54 MHz) δ 49.3 (s). *m/z*: 329.3352 ($C_{21}H_{46}P^+$, 100%).

Tri-*tert*-butyl(nonyl)phosphonium tetrafluoroborate (5b)

1.1 g (10.0 mmol) $NaBF_4$ was added to the solution of 2.1 g (5.0 mmol) tri-*tert*-butyl(nonyl)phosphonium bromide in 12 mL. White precipitate was formed, filtered, dissolved in CH_2Cl_2 and dried over $MgSO_4$ overnight. Then solution was filtered and dried *in vacuo*.

White powder: 1.8 g, 87%; mp. 122.0 °C; 1H NMR ($CDCl_3$, 300.13 MHz) δ 2.27 (m, 2H, P- CH_2), 1.89 (m, 2H, P- $CH_2\text{-}CH_2$), 1.63 (d, $^3J_{PH}$ = 13.98 Hz, 27H, $P(C(CH_3)_3)_3$), 1.56 (m, 2H), 1.38-1.21 (m, 10H), 0.88 (t, $^3J_{HH}$ = 6.4 Hz, 3H, $CH_2\text{-}CH_3$). ^{13}C NMR ($CDCl_3$, 75.47 MHz) δ (CDCl₃) δ = 39.3 (d, $^1J_{PC}$ = 29.3 Hz,

$\text{C}(\text{CH}_3)_3$, 31.8 (s, CH_2), 31.7 (d, ${}^3J_{\text{PC}} = 12.4$ Hz, P- $\text{CH}_2\text{-CH}_2\text{-CH}_2$), 29.8 (s, $\text{C}(\text{CH}_3)_3$), 29.3 (s, CH_2), 29.2 (s, CH_2), 25.0 (d, ${}^2J_{\text{PH}} = 6.6$ Hz, P- $\text{CH}_2\text{-CH}_2$), 22.6 (s, $\text{CH}_2\text{-CH}_3$), 18.5 (d, ${}^1J_{\text{PC}} = 35.2$ Hz, P- CH_2), 14.1 (c, $\text{CH}_2\text{-CH}_3$). ${}^{31}\text{P}$ NMR (CDCl_3 , 121.54 MHz) δ 47.67 (s). m/z : 329.3335 ($\text{C}_{21}\text{H}_{46}\text{P}^+$, 100%).

Tri-*tert*-butyl(undecyl)phosphonium bromide (6a)

The mixture of 2.5 g (12.3 mmol) tri-*tert*-butylphosphine and 2.8 mL (12.3 mmol) 1-bromoundecane was stirred for 8 hours at 100°C. The reaction mixture was washed with diethyl ether and dried *in vacuo*.

White powder: 4.6 g, 85%; mp. 95.0 °C; ${}^1\text{H}$ NMR (CDCl_3 , 300.13 MHz) δ 2.49 (m, 2H, P- CH_2), 1.85 (m, 2H, P- $\text{CH}_2\text{-CH}_2$), 1.62 (d, ${}^3J_{\text{PH}} = 13.91$ Hz, 27H, P($\text{C}(\text{CH}_3)_3$)₃), 1.62 (m, 2H), 1.34-1.15 (m, 12H), 0.81 (t, ${}^3J_{\text{HH}} = 6.67$ Hz, 3H, $\text{CH}_2\text{-CH}_3$). ${}^{13}\text{C}$ NMR (CDCl_3 , 75.47 MHz) δ 39.3 (d, ${}^1J_{\text{PC}} = 29.5$ Hz, $\text{C}(\text{CH}_3)_3$), 31.9 (d, ${}^3J_{\text{PC}} = 12.5$ Hz, P- $\text{CH}_2\text{-CH}_2\text{-CH}_2$), 31.8 (s, CH_2), 30.1 (s, $\text{C}(\text{CH}_3)_3$), 29.5 (m, CH_2), 29.3 (m, CH_2), 25.2 (d, ${}^2J_{\text{PC}} = 6.5$ Hz, P- $\text{CH}_2\text{-CH}_2$), 22.6 (s, $\text{CH}_2\text{-CH}_3$), 19.0 (d, ${}^1J_{\text{PC}} = 34.4$ Hz, P- CH_2), 14.1 (s, $\text{CH}_2\text{-CH}_3$). ${}^{31}\text{P}$ NMR (CDCl_3 , 121.54 MHz) δ 50.6 (s). m/z : 357.3655 ($\text{C}_{23}\text{H}_{50}\text{P}^+$, 100%).

Tri-*tert*-butyl(undecyl)phosphonium tetrafluoroborate (6b)

0.8 g (6.9 mmol) NaBF_4 was added to the solution of 1.5 g (3.4 mmol) tri-*tert*-butyl(undecyl)phosphonium bromide in 10 mL H_2O . White precipitate was formed, filtered, dissolved in CH_2Cl_2 and dried over MgSO_4 overnight. Then solution was filtered and dried *in vacuo*.

White crystalline powder: 1.2 g, 80%; mp. 111.0 °C. ${}^1\text{H}$ NMR (CDCl_3 , 300.13 MHz) δ 2.28 (m, 2H, P- CH_2), 1.91 (m, 2H, P- $\text{CH}_2\text{-CH}_2$), 1.65 (d, ${}^3J_{\text{PH}} = 13.82$ Hz, 27H, P($\text{C}(\text{CH}_3)_3$)₃), 1.58 (m, 2H), 1.38-1.23 (m, 12H), 0.88 (t, ${}^3J_{\text{HH}} = 6.57$ Hz, 3H, $\text{CH}_2\text{-CH}_3$). ${}^{13}\text{C}$ NMR (CDCl_3 , 75.47 MHz) δ 39.3 (d, ${}^1J_{\text{PC}} = 29.1$ Hz, $\text{C}(\text{CH}_3)_3$), 31.9 (s, CH_2), 31.7 (d, ${}^3J_{\text{PC}} = 12.6$ Hz, P- $\text{CH}_2\text{-CH}_2\text{-CH}_2$), 29.8 (s, $\text{C}(\text{CH}_3)_3$), 29.6 (s, CH_2), 29.4 (s, CH_2), 29.3 (s, CH_2), 29.2 (s, CH_2), 25.1 (d, ${}^2J_{\text{PC}} = 6.6$ Hz, P- $\text{CH}_2\text{-CH}_2$), 22.7 (s, $\text{CH}_2\text{-CH}_3$), 18.5 (d, ${}^1J_{\text{PC}} = 34.9$ Hz, P- CH_2), 14.1 (s, $\text{CH}_2\text{-CH}_3$). ${}^{31}\text{P}$ NMR (CDCl_3 , 121.54 MHz) δ 48.9 (s). m/z : 357.3642 ($\text{C}_{23}\text{H}_{50}\text{P}^+$, 100%).

Tri-*tert*-butyl(tridecyl)phosphonium bromide (7a)

The mixture of 2.3 g (11.1 mmol) tri-*tert*-butylphosphine and 2.8 mL (11.1 mmol) 1-bromotridecane was stirred for 8 hours at 100°C. The reaction mixture was washed with diethyl ether (4 X 15 mL) and dried *in vacuo*.

White amorphous powder: 4.2 g, 80%; mp. 72.0 °C; ${}^1\text{H}$ NMR (CDCl_3 , 300.13 MHz) δ 2.46 (m, 2H, P- CH_2), 1.83 (m, 2H, P- $\text{CH}_2\text{-CH}_2$), 1.59 (m, 2H), 1.59 (d, ${}^3J_{\text{PH}} = 13.95$ Hz, 27H, P($\text{C}(\text{CH}_3)_3$)₃), 1.28-1.11 (m, 18H), 0.78 (t, ${}^3J_{\text{HH}} = 6.62$ Hz, 3H, $\text{CH}_2\text{-CH}_3$). ${}^{13}\text{C}$ NMR (CDCl_3 , 75.47 MHz) δ 39.7 (d, ${}^1J_{\text{PC}} = 29.2$ Hz, $\text{C}(\text{CH}_3)_3$), 31.8 (d, ${}^3J_{\text{PC}} = 12.4$ Hz, P- $\text{CH}_2\text{-CH}_2\text{-CH}_2$), 31.8 (s, CH_2), 30.0 (s, $\text{C}(\text{CH}_3)_3$), 29.5 (s, CH_2), 29.4-29.2 (m, CH_2), 25.1 (d, ${}^2J_{\text{PC}} = 7.0$ Hz, P- $\text{CH}_2\text{-CH}_2$), 22.6 (s, $\text{CH}_2\text{-CH}_3$), 19.0 (d, ${}^1J_{\text{PC}} = 34.2$ Hz, P- CH_2), 14.1 (s, $\text{CH}_2\text{-CH}_3$). ${}^{31}\text{P}$ NMR (CDCl_3 , 121.54 MHz) δ 50.7 (s). m/z : 385.3989 ($\text{C}_{25}\text{H}_{54}\text{P}^+$, 100%).

Tri-*tert*-butyl(tridecyl)phosphonium tetrafluoroborate (7b)

0.8 g (6.9 mmol) NaBF_4 was added to the solution of 1.6 g (3.4 mmol) tri-*tert*-butyl(tridecyl)phosphonium bromide in 10 mL H_2O . White precipitate was formed, filtered, dissolved in CH_2Cl_2 and dried over MgSO_4 overnight. Then solution was filtered and dried *in vacuo*.

White crystalline powder: 1.5 g, 91%; mp. 117.0 °C; ${}^1\text{H}$ NMR (CDCl_3 , 300.13 MHz) δ 2.26 (m, 2H, P- CH_2), 1.89 (m, 2H, P- $\text{CH}_2\text{-CH}_2$), 1.62 (d, ${}^3J_{\text{PH}} = 14.05$ Hz, 27H, P($\text{C}(\text{CH}_3)_3$)₃), 1.55 (m, 2H), 1.37-1.20 (m, 18H), 0.86 (t, ${}^3J_{\text{HH}} = 6.72$ Hz, 3H, $\text{CH}_2\text{-CH}_3$). ${}^{13}\text{C}$ NMR (CDCl_3 , 75.47 MHz) δ 39.3 (d, ${}^1J_{\text{PC}} = 29.4$ Hz, $\text{C}(\text{CH}_3)_3$), 31.9 (s, CH_2), 31.7 (d, ${}^3J_{\text{PC}} = 12.6$ Hz, P- $\text{CH}_2\text{-CH}_2\text{-CH}_2$), 29.8 (s, $\text{C}(\text{CH}_3)_3$), 29.6 (s, CH_2), 29.3 (s, CH_2), 29.2 (s, CH_2), 25.0 (d, ${}^2J_{\text{PC}} = 6.7$ Hz, P- $\text{CH}_2\text{-CH}_2$), 22.7 (s, $\text{CH}_2\text{-CH}_3$), 18.5 (d, ${}^1J_{\text{PC}} = 35.0$ Hz, P- CH_2), 14.1 (s, $\text{CH}_2\text{-CH}_3$). ${}^{31}\text{P}$ NMR (CDCl_3 , 121.54 MHz) δ 48.9 (s). m/z : 385.3956 ($\text{C}_{25}\text{H}_{54}\text{P}^+$, 100%).

Tri-*tert*-butyl(pentadecyl)phosphonium bromide (8a)

2.5 g (12.5 mmol) tri-*tert*-butylphosphine and 3.6 g (12.5 mmol) 1-bromopentadecane were dissolved in 10 mL acetonitrile. Reaction mixture was stirred for 10 hours at 100°C in inert atmosphere. Cooled mixture was evaporated and washed with diethyl ether (4 X 20 mL) and dried *in vacuo*.

White amorphous powder: 5.3 g, 86%; mp. 83.0 °C; ${}^1\text{H}$ NMR (CDCl_3 , 300.13 MHz) δ 2.50 (m, 2H, P- CH_2), 1.86 (m, 2H, P- $\text{CH}_2\text{-CH}_2$), 1.63 (d, ${}^3J_{\text{PH}} = 13.66$ Hz, 27H, P($\text{C}(\text{CH}_3)_3$)₃), 1.63 (m, 2H), 1.32-1.15 (m, 22H), 0.81 (t, ${}^3J_{\text{HH}} = 6.61$ Hz, 3H, $\text{CH}_2\text{-CH}_3$). ${}^{13}\text{C}$ NMR (CDCl_3 , 75.47 MHz) δ 39.3 (d, ${}^1J_{\text{PC}} = 29.7$ Hz, $\text{C}(\text{CH}_3)_3$), 31.9 (d, ${}^3J_{\text{PC}} = 12.7$ Hz, P- $\text{CH}_2\text{-CH}_2\text{-CH}_2$), 31.9 (s, CH_2), 30.1 (s, $\text{C}(\text{CH}_3)_3$), 29.6 (m, CH_2), 29.3 (m, CH_2),

25.2 (d, $^2J_{PC} = 6.6$ Hz, P-CH₂-CH₂), 22.6 (s, CH₂-CH₃), 19.0 (d, $^1J_{PC} = 34.4$ Hz, P-CH₂), 14.1 (s, CH₂-CH₃). ^{31}P NMR (CDCl₃, 121.54 MHz) δ 50.6 (s). *m/z*: 413.4332 (C₂₇H₅₈P⁺, 100%).

Tri-*tert*-butyl(pentadecyl)phosphonium tetrafluoroborate (8b)

1.5 g (3.1 mmol) tri-*tert*-butyl(pentadecyl)phosphonium bromide was dissolved in 15 mL of water. 0.7 g (6.2 mmol) NaBF₄ was added to the solution. White precipitate was formed, it was filtered, dissolved in CH₂Cl₂ and dried over MgSO₄ overnight. Then solution was filtered and evaporated *in vacuo*.

White powder: 1.4 g, 90%; mp. 130.0°C; 1H NMR (CDCl₃, 300.13 MHz) δ 2.27 (m, 2H, P-CH₂), 1.90 (m, 2H, P-CH₂-CH₂), 1.63 (d, $^3J_{PH} = 13.91$ Hz, 27H, P(C(CH₃)₃)₃), 1.56 (m, 2H), 1.38-1.20 (m, 22H), 0.87 (t, $^3J_{HH} = 6.62$ Hz, 3H, CH₂-CH₃). ^{13}C NMR (CDCl₃, 75.47 MHz) δ 39.3 (d, $^1J_{PC} = 29.4$ Hz, C(CH₃)₃), 31.9 (s, CH₂), 31.7 (d, $^3J_{PC} = 12.6$ Hz, P-CH₂-CH₂-CH₂), 29.8 (s, C(CH₃)₃), 29.7-29.5 (m, CH₂), 29.4 (m, CH₂), 29.2 (s, CH₂), 25.0 (d, $^2J_{PC} = 6.7$ Hz, P-CH₂-CH₂), 22.7 (s, CH₂-CH₃), 18.5 (d, $^1J_{PC} = 35.2$ Hz, P-CH₂), 14.1 (s, CH₂-CH₃). ^{31}P NMR (CDCl₃, 121.54 MHz) δ 48.8 (s). *m/z*: 413.4268 (C₂₇H₅₈P⁺, 100%).

Tri-*tert*-butyl(heptadecyl)phosphonium bromide (9a)

The mixture of 1.3 g (6.5 mmol) tri-*tert*-butylphosphine and 2.1 g (6.5 mmol) 1-bromoheptadecane were dissolved in 15 mL DMF. Reaction mixture was stirred for 10 hours at 100°C in inert atmosphere. After cooling the reaction solvent was removed in vacuum. The solid was washed with diethyl ether (4 X 10 mL) and dried *in vacuo*.

White amorphous powder: 2.2 g, 64%; mp. 93.0°C; 1H NMR (CDCl₃, 300.13 MHz) δ 2.48 (m, 2H, P-CH₂), 1.85 (m, 2H, P-CH₂-CH₂), 1.61 (d, $^3J_{PH} = 13.85$ Hz, 27H, P(C(CH₃)₃)₃), 1.60 (m, 2H), 1.31-1.13 (m, 26H), 0.80 (t, $^3J_{HH} = 6.52$ Hz, 3H, CH₂-CH₃). ^{13}C NMR (CDCl₃, 75.5 MHz) δ 39.3 (d, $^1J_{PC} = 29.4$ Hz, C(CH₃)₃), 31.9 (d, $^3J_{PC} = 12.6$ Hz, P-CH₂-CH₂-CH₂), 31.8 (s, CH₂), 30.1 (s, C(CH₃)₃), 29.6 (m, CH₂), 29.3 (m, CH₂), 25.2 (d, $^2J_{PC} = 6.7$ Hz, P-CH₂-CH₂), 22.6 (s, CH₂-CH₃), 19.0 (d, $^1J_{PC} = 34.4$ Hz, P-CH₂), 14.1 (s, CH₂-CH₃). ^{31}P NMR (CDCl₃, 121.54 MHz) δ 50.6 (s). *m/z*: 441.4596 (C₂₉H₆₂P⁺, 100%).

Tri-*tert*-butyl(heptadecyl)phosphonium tetrafluoroborate (9b)

0.9 g (1.8 mmol) of tri-*tert*-butyl(heptadecyl)phosphonium bromide was dissolved in 10 mL of water. 0.4 g (3.5 mmol) NaBF₄ was added to the solution. White precipitate was formed, it was filtered, dissolved in CH₂Cl₂ and dried over MgSO₄ overnight. Then solution was filtered and evaporated *in vacuo*.

Yellowish amorphous powder: 0.9 g, 91%; mp. 140.0°C; 1H NMR (CDCl₃, 300.13 MHz) δ 2.26 (m, 2H, P-CH₂), 1.86 (m, 2H, P-CH₂-CH₂), 1.63 (d, $^3J_{PH} = 13.94$ Hz, 27H, P(C(CH₃)₃)₃), 1.55 (m, 2H), 1.36-1.21 (m, 26H), 0.86 (t, $^3J_{HH} = 6.57$ Hz, 3H, CH₂-CH₃). ^{13}C NMR (CDCl₃, 75.47 MHz) δ 39.3 (d, $^1J_{PC} = 29.6$ Hz, C(CH₃)₃), 31.9 (s, CH₂), 31.7 (d, $^3J_{PC} = 12.5$ Hz, P-CH₂-CH₂-CH₂), 29.8 (s, C(CH₃)₃), 29.7-29.5 (m, CH₂), 29.4-29.3 (s, CH₂), 29.2 (s, CH₂), 25.0 (d, $^2J_{PC} = 6.5$ Hz, P-CH₂-CH₂), 22.7 (s, CH₂-CH₃), 18.5 (d, $^1J_{PC} = 35.1$ Hz, P-CH₂), 14.1 (s, CH₂-CH₃). ^{31}P NMR (CDCl₃, 121.54 MHz) δ 48.8 (s). *m/z*: 441.4581 (C₂₉H₆₂P⁺, 100%).

X-ray crystallographic data and refinement details

X-ray diffraction data for **2b**, **2b'**, **3b** and **4b** (model **4b_A**) were collected on a Bruker Quest D8 diffractometer equipped with a Photon-III area-detector (shutterless φ - and ω -scan technique), using graphite-monochromatized Mo K α -radiation ($\lambda=0.71073\text{\AA}$). The intensity data were integrated by the SAINT program¹ and semi-empirically corrected from equivalent reflections for absorption and decay with SADABS.² Since crystal **4b** were needles of a very small diameter and demonstrated poor scattering, its crystallographic model **4b_A** exhibited some problems. Therefore, X-ray diffraction data for **4b** (model **4b_B**) were recollected at 100K on a four-circle Rigaku Synergy S diffractometer equipped with a HyPix600HE area-detector (kappa geometry, shutterless ω -scan technique), using graphite monochromatized Cu K α -radiation ($\lambda=1.54184\text{\AA}$); the intensity data were integrated and corrected for absorption and decay by the CrysAlisPro program.³ All structures were solved by direct methods using SHELXT⁴ and refined by the full-matrix least-squares on F^2 using SHELXL-2018⁵ or OLEX2 for **4b_B**.⁶ All non-hydrogen atoms were refined with anisotropic displacement parameters. All hydrogen atoms were placed in ideal calculated positions (C-H distance = 0.950 Å for aromatic, 0.980 Å for methyl, 0.990 Å for methylene and 1.000 Å for tertiary hydrogen atoms) and refined as riding atoms with relative isotropic displacement parameters defined as $U_{\text{iso}}(\text{H})=1.5 U_{\text{eq}}(\text{C})$ for methyl, 1.2 $U_{\text{eq}}(\text{C})$ otherwise. A rotating group model was applied for methyl groups. The disordered fragments were modeled by applying similarity constraints on anisotropic displacement parameters on similar atoms and by constraining similar distances to be equal within the deviation of 0.003Å. Crystal data, data collection and structure refinement details are summarized in Table S1.

Literature references:

1. Bruker. APEX-III. *Bruker AXS Inc.*, Madison, Wisconsin, USA, **2019**.
2. Krause, L.; Herbst-Irmer, R.; Sheldrick, G. M.; Stalke, D. Comparison of silver and molybdenum microfocus X-ray sources for single-crystal structure determination. *J. Appl. Cryst.* **2015**, *48*, 3-10. <http://doi.org/10.1107/S1600576714022985>
3. CrysAlisPro. Version 1.171.41.106a. *Rigaku Oxford Diffraction*, **2021**.
4. Sheldrick, G. M. SHELXT - Integrated space-group and crystal-structure determination. *Acta Cryst.* **2015**, *A71*, 3-8. <http://doi.org/10.1107/S2053273314026370>
5. Sheldrick, G. M. Crystal structure refinement with SHELXL. *Acta Cryst.* **2015**, *C71*, 3-8. <http://doi.org/10.1107/S2053229614024218>
6. Dolomanov O.V.; Bourhis L.J.; Gildea R.J.; Howard J.A.K.; Puschmann H. OLEX2: a complete structure solution, refinement and analysis program. *J. Appl. Cryst.* **2009**, *42*(2), 229-341. <http://doi.org/10.1107/S0021889808042726>

Table S1. Crystal data and structure refinement for **2b**.

Identification code	2b	2b'	3b	4b_A	4b_B
Formula	[P ^t Bu ₃ nPr] ⁺ [BF ₄] ⁻	[P ^t Bu ₃ nPr] ⁺ [BF ₄] ⁻ _{0.96} I _{0.04}	[P ^t Bu ₃ (n-C ₅ H ₁₁)] ⁺ [BF ₄] ⁻	[P ^t Bu ₃ (n-C ₇ H ₁₅)] ⁺ [BF ₄] ⁻	[P ^t Bu ₃ (n-C ₇ H ₁₅)] ⁺ [BF ₄] ⁻
Empirical formula	C ₁₅ H ₃₄ BF ₄ P	C ₁₅ H ₃₄ B _{0.96} F _{3.85} I _{0.04} P	C ₁₇ H ₃₈ BF ₄ P	C ₁₉ H ₄₂ BF ₄ P	C ₁₉ H ₄₂ BF ₄ P
Formula weight	332.20	333.75	360.25	388.30	388.30
Temperature / K	100(2)	100(2)	100(2)	100(2)	100.0(1)
Wavelength / Å	0.71073	0.71073	0.71073	0.71073	1.54184
Crystal system	Monoclinic	Monoclinic	Orthorhombic	Monoclinic	Monoclinic
Space group	P2 ₁ /n	P2 ₁ /n	Pbca	P2 ₁ /c	P2 ₁ /c
Unit cell dimensions					
a / Å	8.14660(10)	8.1440(2) Å	20.3681(5)	11.9983(2)	12.00390(10)
b / Å	14.7947(3)	14.7851(4) Å	16.6259(4)	41.8792(8)	41.9558(3)
c / Å	15.2565(3)	15.2423(3) Å	35.6517(9)	17.7093(3)	17.73890(10)
β / °	95.4414(6)	95.4434(6)	90°	90.9046(10)	90.9060(10)
Volume / Å ³	1830.53(6)	1827.05(8)	12073.0(5)	8897.4(3)	8932.78(11)
Z	4	4	24	16	16
Density (calcd) / g•cm ⁻³	1.205	1.213	1.189	1.160	1.155
μ / mm ⁻¹	0.178	0.242	0.167	0.156	1.370
F(000)	720	721.9	4704	3392	3392
Crystal size / mm	0.36 x 0.19 x 0.15	0.59 x 0.30 x 0.24	0.59 x 0.21 x 0.13	0.49 x 0.06 x 0.05	0.28 x 0.02 x 0.02
θ range / °	1.922 to 34.997	2.685 to 34.350	2.285 to 34.350	2.093 to 31.500	2.705 to 77.841
Index ranges	-13<=h<=13, -23<=k<=23, -24<=l<=24	-12<=h<=12, -23<=k<=23, -24<=l<=24	-32<=h<=32, -26<=k<=26, -56<=l<=56	-17<=h<=17, -61<=k<=61, -26<=l<=26	-14<=h<=13, -53<=k<=52, -22<=l<=22

Table S1 (cont.). Crystal data and structure refinement for **2b**.

Identification code	2b	2b'	3b	4b_A	4b_B
Reflections					
collected	70308	62120	378459	245680	83912
independent [R _{int}]	8057 [0.0409]	7654 [0.0435]	25281 [0.0449]	29592 [0.1829]	17948 [0.0696]
observed (I>2σ(I))	6918	6331	20391	15329	14986
Completeness to θ _{full} , θ _{max}	0.998, 0.999	1.000, 1.000	0.999, 0.999	0.999, 0.999	0.972, 0.941
Max., min. transmission	0.8625, 0.8368	0.8022, 0.7370	0.8625, 0.7983	0.8020, 0.7030	1.00000, 0.28801
Data, restraints, parameters	8057, 26, 216	7654, 6, 204	25281, 0, 652	29592, 745, 1236	17948, 745, 1238
Goodness-of-fit on F ²	1.023	1.041	1.023	1.065	1.042
R1, wR2 indices (I>2σ(I))	0.0316, 0.0813	0.0426, 0.1015	0.0413, 0.0999	0.0941, 0.2144	0.0673, 0.1820
R1, wR2 indices (all data)	0.0398, 0.0877	0.0558, 0.1110	0.0561, 0.1118	0.1853, 0.2677	0.0767, 0.1883
Δρ(ē) max, min / ē·Å ⁻³	0.449, -0.262	0.509, -0.370	0.659, -0.443	0.599, -0.523	0.466, -0.344
CCDC deposition code	2099141	2099142	2099143	2099144	2099145

The structure of **2b / [^tBu₃P(*n*-C₃H₇)]⁺[BF₄]⁻**

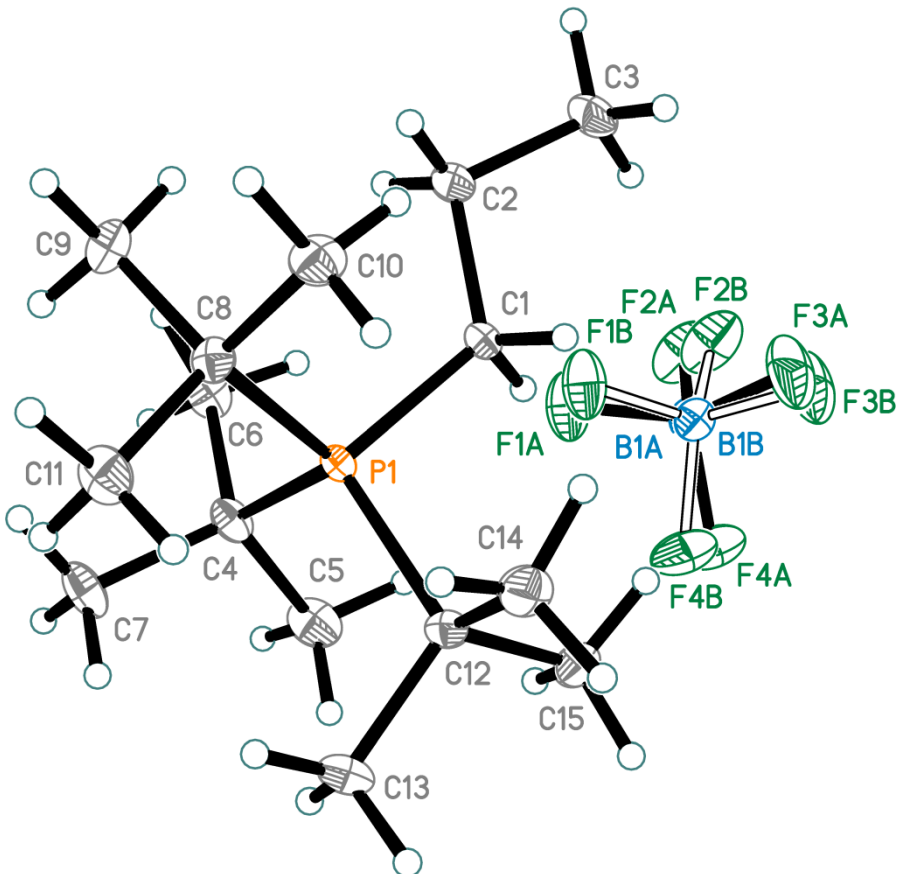


Figure S1. The structure of **2b**. The [BF₄]⁻ anion is disordered over two positions (*A* and *B*) with the disorder ratio of 0.855(9):0.145(9). The displacement ellipsoids are set to the 50% probability level.

Table S2. Bond lengths for **2b** / Å.

Bond	Distance	Bond	Distance	Bond	Distance
P(1)-C(1)	1.8216(6)	C(4)-C(6)	1.5445(10)	F(1A)-B(1A)	1.394(3)
P(1)-C(4)	1.8793(7)	C(8)-C(11)	1.5420(10)	F(2A)-B(1A)	1.392(3)
P(1)-C(8)	1.8804(7)	C(8)-C(9)	1.5438(10)	F(3A)-B(1A)	1.386(3)
P(1)-C(12)	1.8835(7)	C(8)-C(10)	1.5444(10)	F(4A)-B(1A)	1.398(3)
C(1)-C(2)	1.5388(9)	C(12)-C(13)	1.5391(10)	F(1B)-B(1B)	1.369(14)
C(2)-C(3)	1.5240(10)	C(12)-C(14)	1.5442(10)	F(2B)-B(1B)	1.357(14)
C(4)-C(7)	1.5396(10)	C(12)-C(15)	1.5443(10)	F(3B)-B(1B)	1.355(14)
C(4)-C(5)	1.5421(11)			F(4B)-B(1B)	1.368(14)

Table S3. Bond angles for **2b** / °.

Bond angle	Value	Bond angle	Value	Bond angle	Value
C(1)-P(1)-C(4)	108.18(3)	C(6)-C(4)-P(1)	110.22(5)	F(3A)-B(1A)-F(2A)	112.7(2)
C(1)-P(1)-C(8)	109.42(3)	C(11)-C(8)-C(9)	108.00(6)	F(3A)-B(1A)-F(1A)	108.9(2)
C(4)-P(1)-C(8)	112.01(3)	C(11)-C(8)-C(10)	108.01(6)	F(2A)-B(1A)-F(1A)	108.6(2)
C(1)-P(1)-C(12)	103.27(3)	C(9)-C(8)-C(10)	107.08(6)	F(3A)-B(1A)-F(4A)	109.7(2)

C(4)-P(1)-C(12)	111.61(3)	C(11)-C(8)-P(1)	112.50(5)	F(2A)-B(1A)-F(4A)	106.5(2)
C(8)-P(1)-C(12)	111.90(3)	C(9)-C(8)-P(1)	110.97(5)	F(1A)-B(1A)-F(4A)	110.3(2)
C(2)-C(1)-P(1)	122.47(5)	C(10)-C(8)-P(1)	110.08(5)	F(3B)-B(1B)-F(2B)	96.1(13)
C(3)-C(2)-C(1)	108.82(6)	C(13)-C(12)-C(14)	108.06(6)	F(3B)-B(1B)-F(4B)	108.9(13)
C(7)-C(4)-C(5)	107.97(6)	C(13)-C(12)-C(15)	109.03(6)	F(2B)-B(1B)-F(4B)	126.1(15)
C(7)-C(4)-C(6)	109.39(6)	C(14)-C(12)-C(15)	106.05(6)	F(3B)-B(1B)-F(1B)	112.5(13)
C(5)-C(4)-C(6)	104.88(6)	C(13)-C(12)-P(1)	112.50(5)	F(2B)-B(1B)-F(1B)	111.4(12)
C(7)-C(4)-P(1)	112.15(5)	C(14)-C(12)-P(1)	111.00(5)	F(4B)-B(1B)-F(1B)	101.9(12)
C(5)-C(4)-P(1)	111.96(5)	C(15)-C(12)-P(1)	109.97(5)		

The structure of **2b'** / $[^t\text{Bu}_3\text{P}(n\text{-C}_3\text{H}_7)]^+[\text{BF}_4]^-0.96\text{I}^-0.04$

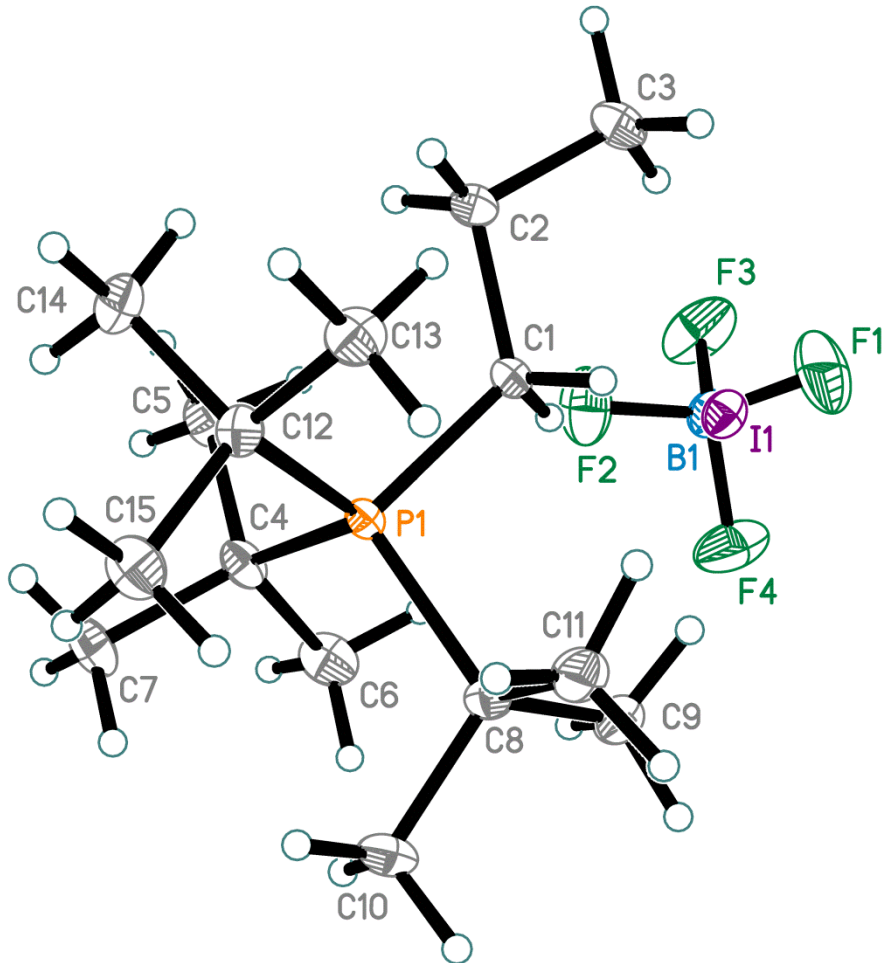


Figure S2. The structure of **2b'**. The disorder ratio for the $[\text{BF}_4]^- / \text{I}^-$ positional disorder is 0.9614(4):0.0386(4). The displacement ellipsoids are set to the 50% probability level.

The distance between boron and iodine positions is 0.171 Å. The additional disorder of the $[\text{BF}_4]^-$ anion is not resolved.

Table S4. Bond lengths for **2b'** / Å.

Bond	Distance	Bond	Distance	Bond	Distance
F(1)-B(1)	1.3851(19)	P(1)-C(8)	1.8841(10)	C(8)-C(10)	1.5388(14)
F(2)-B(1)	1.3850(19)	C(1)-C(2)	1.5384(13)	C(8)-C(11)	1.5416(14)
F(3)-B(1)	1.3846(19)	C(2)-C(3)	1.5227(14)	C(8)-C(9)	1.5434(15)

F(4)-B(1)	1.3849(19)	C(4)-C(7)	1.5395(14)	C(12)-C(15)	1.5408(14)
P(1)-C(1)	1.8207(9)	C(4)-C(6)	1.5406(15)	C(12)-C(14)	1.5432(14)
P(1)-C(4)	1.8793(9)	C(4)-C(5)	1.5448(14)	C(12)-C(13)	1.5439(14)
P(1)-C(12)	1.8798(9)				

Table S5. Bond angles for **2b'** / °.

Bond angle	Value	Bond angle	Value	Bond angle	Value
F(3)-B(1)-F(4)	108.53(14)	C(12)-P(1)-C(8)	111.90(4)	C(11)-C(8)-C(9)	106.09(9)
F(3)-B(1)-F(2)	109.30(14)	C(2)-C(1)-P(1)	122.45(7)	C(10)-C(8)-P(1)	112.42(7)
F(4)-B(1)-F(2)	110.19(15)	C(3)-C(2)-C(1)	108.91(8)	C(11)-C(8)-P(1)	110.92(7)
F(3)-B(1)-F(1)	110.48(15)	C(7)-C(4)-C(6)	108.10(8)	C(9)-C(8)-P(1)	109.90(7)
F(4)-B(1)-F(1)	109.16(15)	C(7)-C(4)-C(5)	109.35(8)	C(15)-C(12)-C(14)	108.03(8)
F(2)-B(1)-F(1)	109.18(14)	C(6)-C(4)-C(5)	104.94(8)	C(15)-C(12)-C(13)	107.98(8)
C(1)-P(1)-C(4)	108.19(4)	C(7)-C(4)-P(1)	112.13(6)	C(14)-C(12)-C(13)	107.14(8)
C(1)-P(1)-C(12)	109.43(4)	C(6)-C(4)-P(1)	111.93(7)	C(15)-C(12)-P(1)	112.45(7)
C(4)-P(1)-C(12)	112.04(4)	C(5)-C(4)-P(1)	110.11(7)	C(14)-C(12)-P(1)	110.95(6)
C(1)-P(1)-C(8)	103.26(4)	C(10)-C(8)-C(11)	108.21(8)	C(13)-C(12)-P(1)	110.10(7)
C(4)-P(1)-C(8)	111.58(4)	C(10)-C(8)-C(9)	109.08(8)		

The structure of **3b / [^tBu₃P(*n*-C₅H₁₁)]⁺[BF₄]⁻**

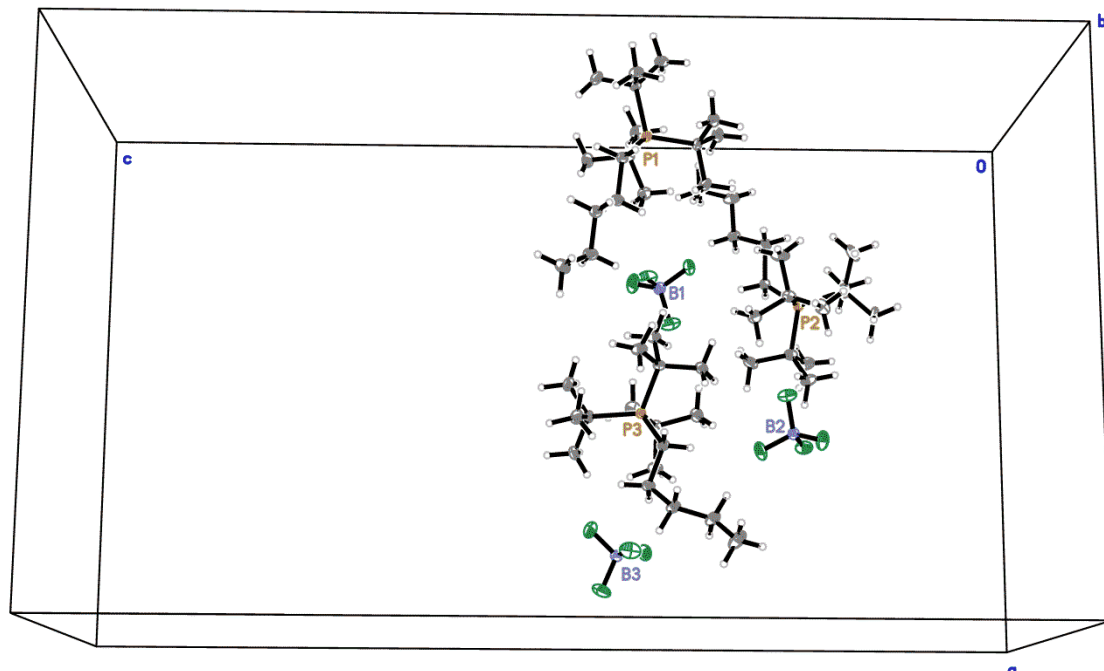


Figure S3. Crystallographically non-equivalent ions of **3b**. The displacement ellipsoids are set to the 50% probability level.

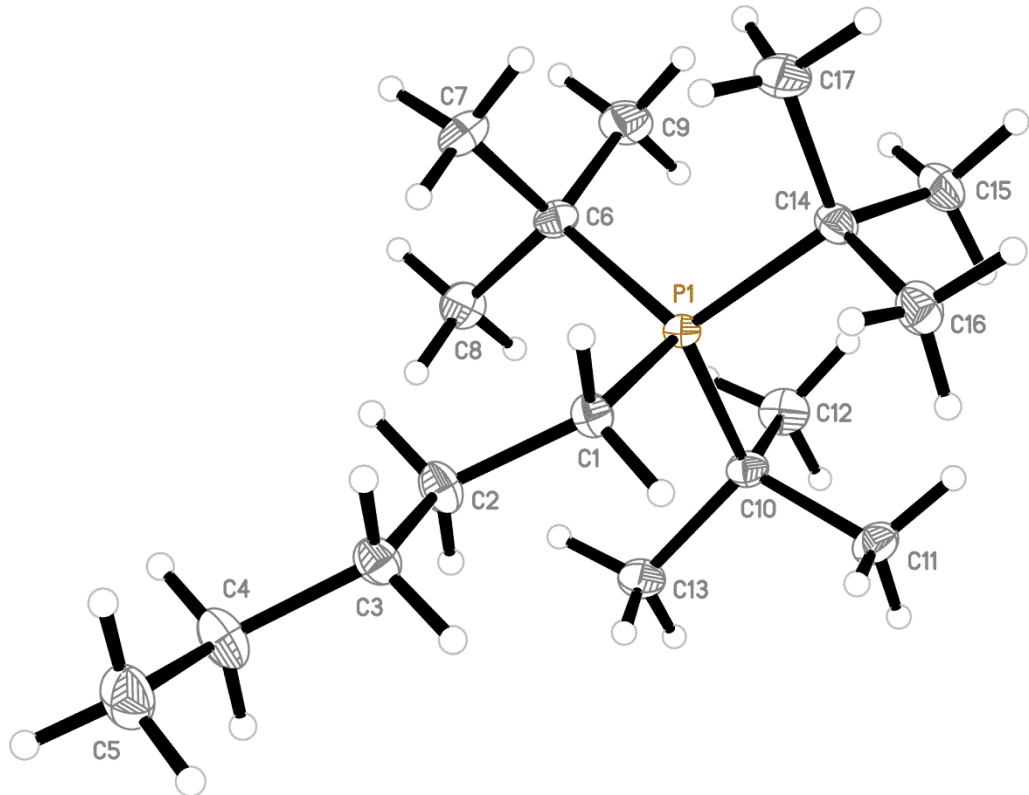


Figure S4. The first crystallographically non-equivalent cation $[{}^t\text{Bu}_3\text{P}(n\text{-C}_5\text{H}_{11})]^+$ in **3b**. The displacement ellipsoids are set to the 50% probability level.

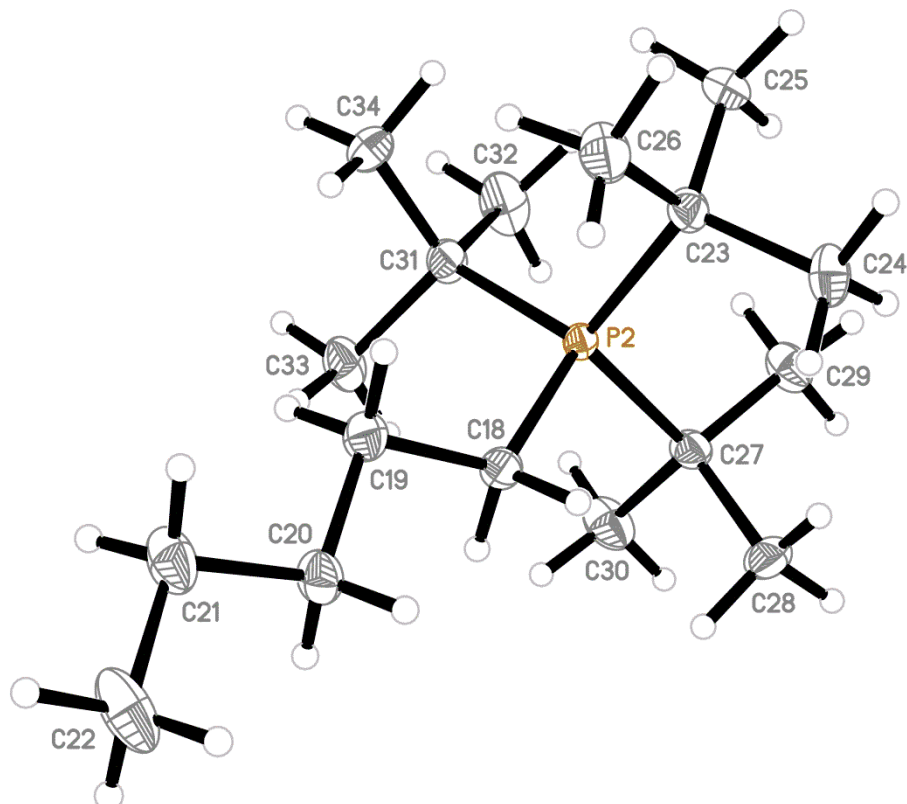


Figure S5. The second crystallographically non-equivalent cation $[{}^t\text{Bu}_3\text{P}(n\text{-C}_5\text{H}_{11})]^+$ in **3b**. The displacement ellipsoids are set to the 50% probability level.

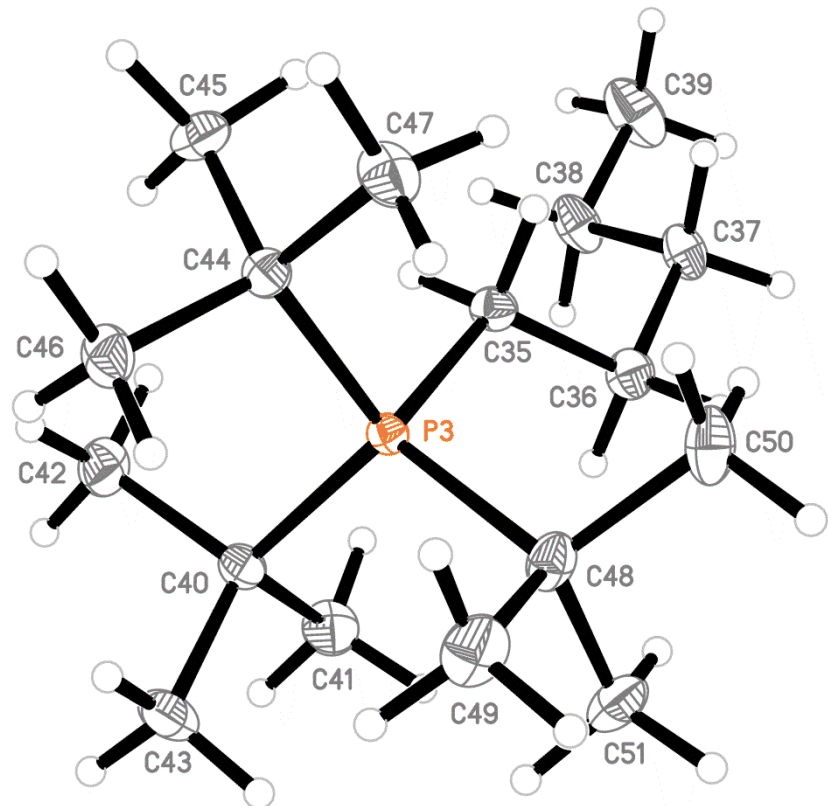


Figure S6. The third crystallographically non-equivalent cation $[{}^t\text{Bu}_3\text{P}(n\text{-C}_5\text{H}_{11})]^+$ in **3b**. The displacement ellipsoids are set to the 50% probability level.

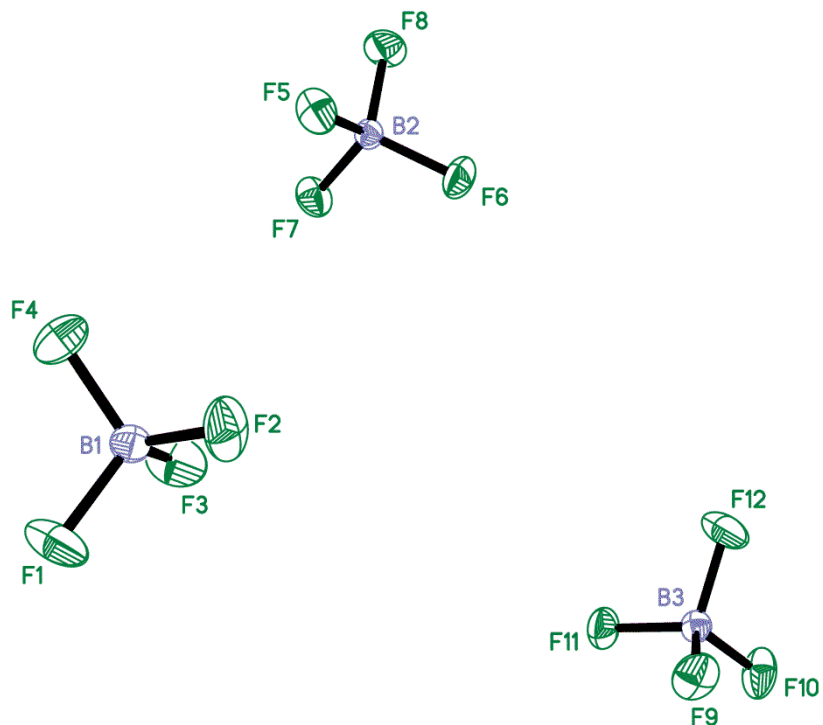


Figure S7. Three crystallographically non-equivalent anions $[\text{BF}_4]^-$ in **3b**. The displacement ellipsoids are set to the 50% probability level.

Table S6. Bond lengths for **3b** / Å.

Bond	Distance	Bond	Distance	Bond	Distance
P(1)-C(1)	1.8226(8)	P(2)-C(18)	1.8198(9)	P(3)-C(35)	1.8252(8)

P(1)-C(6)	1.8810(9)	P(2)-C(23)	1.8775(9)	P(3)-C(40)	1.8801(9)
P(1)-C(10)	1.8770(8)	P(2)-C(27)	1.8877(9)	P(3)-C(44)	1.8823(9)
P(1)-C(14)	1.8896(9)	P(2)-C(31)	1.8768(9)	P(3)-C(48)	1.8780(9)
C(1)-C(2)	1.5396(12)	C(18)-C(19)	1.5329(13)	C(35)-C(36)	1.5420(12)
C(2)-C(3)	1.5236(13)	C(19)-C(20)	1.5265(14)	C(36)-C(37)	1.5322(13)
C(3)-C(4)	1.5208(13)	C(20)-C(21)	1.5189(14)	C(37)-C(38)	1.5236(13)
C(4)-C(5)	1.5152(14)	C(21)-C(22)	1.5172(17)	C(38)-C(39)	1.5234(15)
C(6)-C(9)	1.5398(14)	C(23)-C(25)	1.5371(15)	C(40)-C(43)	1.5383(14)
C(6)-C(8)	1.5422(13)	C(23)-C(24)	1.5399(14)	C(40)-C(42)	1.5411(13)
C(6)-C(7)	1.5441(13)	C(23)-C(26)	1.5444(14)	C(40)-C(41)	1.5412(13)
C(10)-C(12)	1.5382(13)	C(27)-C(29)	1.5365(13)	C(44)-C(47)	1.5375(13)
C(10)-C(11)	1.5409(13)	C(27)-C(28)	1.5397(14)	C(44)-C(46)	1.5395(12)
C(10)-C(13)	1.5421(13)	C(27)-C(30)	1.5429(14)	C(44)-C(45)	1.5445(13)
C(14)-C(17)	1.5414(13)	C(31)-C(32)	1.5352(15)	C(48)-C(49)	1.5416(13)
C(14)-C(15)	1.5420(13)	C(31)-C(34)	1.5430(16)	C(48)-C(51)	1.5418(14)
C(14)-C(16)	1.5438(13)	C(31)-C(33)	1.5452(14)	C(48)-C(50)	1.5447(14)
B(1)-F(2)	1.3864(13)	B(2)-F(5)	1.3948(12)	B(3)-F(9)	1.3860(13)
B(1)-F(1)	1.3945(13)	B(2)-F(6)	1.3902(12)	B(3)-F(10)	1.3926(12)
B(1)-F(3)	1.3940(13)	B(2)-F(7)	1.3900(12)	B(3)-F(11)	1.3986(12)
B(1)-F(4)	1.3888(13)	B(2)-F(8)	1.3923(12)	B(3)-F(12)	1.3818(13)

Table S7. Bond angles for **3b** / °.

Bond angle	Value	Bond angle	Value	Bond angle	Value
C(1)-P(1)-C(10)	108.48(4)	C(18)-P(2)-C(31)	109.41(4)	C(35)-P(3)-C(48)	108.86(4)
C(1)-P(1)-C(6)	108.88(4)	C(18)-P(2)-C(23)	109.07(4)	C(35)-P(3)-C(40)	108.18(4)
C(10)-P(1)-C(6)	112.38(4)	C(31)-P(2)-C(23)	112.49(4)	C(48)-P(3)-C(40)	112.65(4)
C(1)-P(1)-C(14)	104.10(4)	C(18)-P(2)-C(27)	102.89(4)	C(35)-P(3)-C(44)	103.89(4)
C(10)-P(1)-C(14)	110.81(4)	C(31)-P(2)-C(27)	111.70(5)	C(48)-P(3)-C(44)	112.09(4)
C(6)-P(1)-C(14)	111.78(4)	C(23)-P(2)-C(27)	110.83(4)	C(40)-P(3)-C(44)	110.71(4)
C(2)-C(1)-P(1)	121.52(6)	C(19)-C(18)-P(2)	123.22(7)	C(36)-C(35)-P(3)	121.87(6)
C(3)-C(2)-C(1)	110.58(7)	C(20)-C(19)-C(18)	108.90(8)	C(37)-C(36)-C(35)	110.23(7)
C(4)-C(3)-C(2)	112.44(8)	C(21)-C(20)-C(19)	113.43(9)	C(38)-C(37)-C(36)	114.47(8)
C(5)-C(4)-C(3)	113.32(9)	C(22)-C(21)-C(20)	112.63(10)	C(39)-C(38)-C(37)	111.74(8)
C(9)-C(6)-C(8)	107.97(8)	C(25)-C(23)-C(24)	107.96(8)	C(43)-C(40)-C(42)	108.48(8)
C(9)-C(6)-C(7)	108.66(8)	C(25)-C(23)-C(26)	109.97(9)	C(43)-C(40)-C(41)	109.26(8)
C(8)-C(6)-C(7)	107.19(8)	C(24)-C(23)-C(26)	105.33(8)	C(42)-C(40)-C(41)	105.65(8)
C(9)-C(6)-P(1)	112.86(7)	C(25)-C(23)-P(2)	112.04(7)	C(43)-C(40)-P(3)	112.94(7)
C(8)-C(6)-P(1)	110.55(6)	C(24)-C(23)-P(2)	111.66(7)	C(42)-C(40)-P(3)	111.00(6)
C(7)-C(6)-P(1)	109.43(6)	C(26)-C(23)-P(2)	109.65(7)	C(41)-C(40)-P(3)	109.24(6)
C(12)-C(10)-C(11)	108.36(8)	C(29)-C(27)-C(28)	108.84(8)	C(47)-C(44)-C(46)	108.13(7)

C(12)-C(10)-C(13)	108.71(8)	C(29)-C(27)-C(30)	108.08(8)	C(47)-C(44)-C(45)	105.76(8)
C(11)-C(10)-C(13)	105.61(7)	C(28)-C(27)-C(30)	105.91(9)	C(46)-C(44)-C(45)	109.64(7)
C(12)-C(10)-P(1)	111.83(6)	C(29)-C(27)-P(2)	112.17(7)	C(47)-C(44)-P(3)	111.40(6)
C(11)-C(10)-P(1)	110.88(6)	C(28)-C(27)-P(2)	110.23(7)	C(46)-C(44)-P(3)	112.26(6)
C(13)-C(10)-P(1)	111.22(6)	C(30)-C(27)-P(2)	111.37(7)	C(45)-C(44)-P(3)	109.43(6)
C(17)-C(14)-C(15)	107.34(8)	C(32)-C(31)-C(34)	109.03(9)	C(49)-C(48)-C(51)	107.95(8)
C(17)-C(14)-C(16)	106.33(8)	C(32)-C(31)-C(33)	108.81(9)	C(49)-C(48)-C(50)	108.05(8)
C(15)-C(14)-C(16)	109.53(8)	C(34)-C(31)-C(33)	106.41(9)	C(51)-C(48)-C(50)	107.77(8)
C(17)-C(14)-P(1)	110.72(6)	C(32)-C(31)-P(2)	112.13(7)	C(49)-C(48)-P(3)	111.74(6)
C(15)-C(14)-P(1)	112.37(6)	C(34)-C(31)-P(2)	110.43(7)	C(51)-C(48)-P(3)	110.59(6)
C(16)-C(14)-P(1)	110.33(6)	C(33)-C(31)-P(2)	109.85(7)	C(50)-C(48)-P(3)	110.62(7)
F(2)-B(1)-F(4)	108.58(9)	F(7)-B(2)-F(6)	110.09(8)	F(12)-B(3)-F(9)	109.73(9)
F(2)-B(1)-F(3)	110.40(9)	F(7)-B(2)-F(8)	109.72(8)	F(12)-B(3)-F(10)	109.50(9)
F(4)-B(1)-F(3)	108.91(9)	F(6)-B(2)-F(8)	109.13(8)	F(9)-B(3)-F(10)	109.82(9)
F(2)-B(1)-F(1)	109.78(9)	F(7)-B(2)-F(5)	109.28(8)	F(12)-B(3)-F(11)	109.62(9)
F(4)-B(1)-F(1)	109.25(9)	F(6)-B(2)-F(5)	109.24(8)	F(9)-B(3)-F(11)	108.85(9)
F(3)-B(1)-F(1)	109.89(9)	F(8)-B(2)-F(5)	109.37(8)	F(10)-B(3)-F(11)	109.31(8)

The structure of **4b** / $[{}^t\text{Bu}_3\text{P}(n\text{-C}_7\text{H}_{15})]^+[\text{BF}_4]^-$

The crystallographic models **4b_A** (Mo K α radiation) and **4b_B** (Cu K α radiation) were nearly identical. Geometrical parameters for model **4b_B** is presented below since **4b_A** demonstrated poorer results.

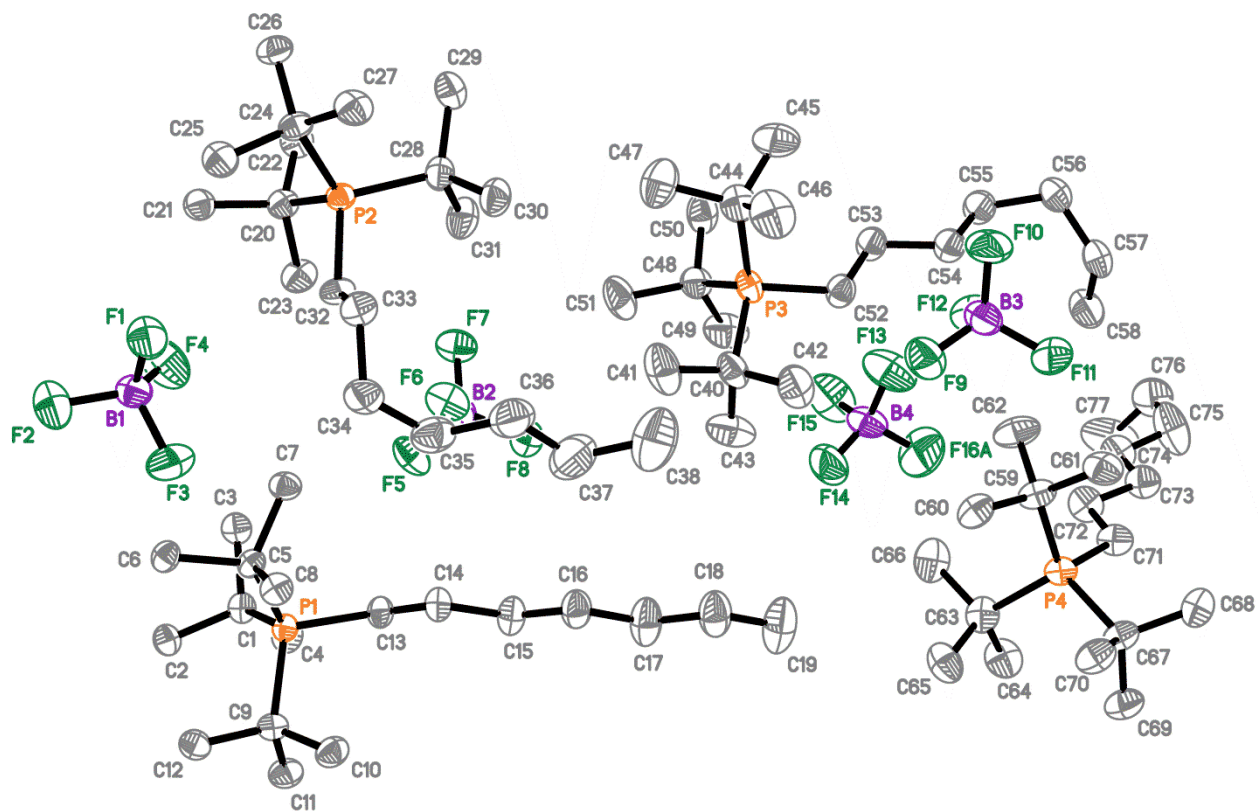


Figure S8. Crystallographically non-equivalent cations $[{}^t\text{Bu}_3\text{P}(n\text{-C}_7\text{H}_{15})]^+$ and anions $[\text{BF}_4]^-$ in **4b**. The disorder is not shown. Hydrogen atoms are omitted. The displacement ellipsoids are set to the 50% probability level.

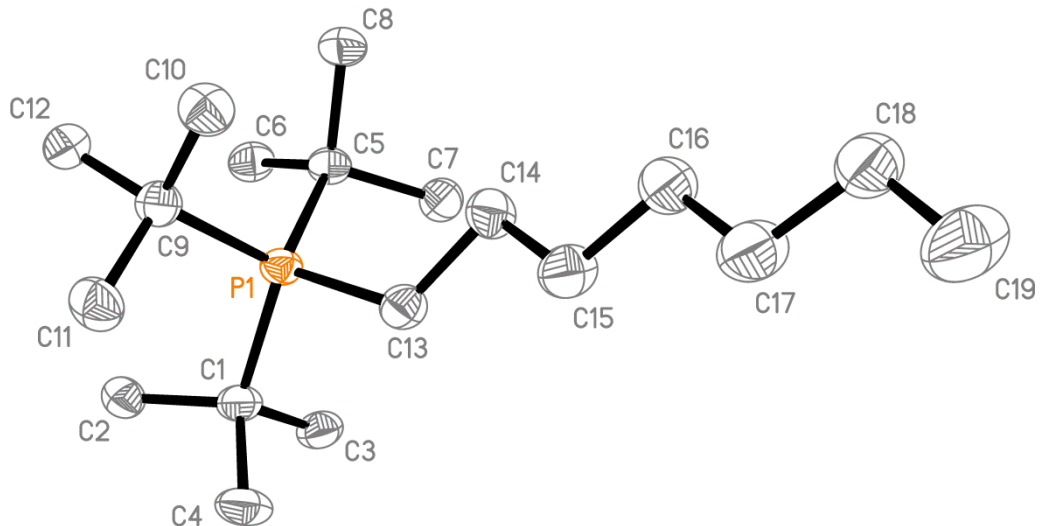


Figure S9. The first crystallographically non-equivalent cation $[{}^t\text{Bu}_3\text{P}(n\text{-C}_7\text{H}_{15})]^+$ in **4b**. Hydrogen atoms are omitted. The displacement ellipsoids are set to the 50% probability level.

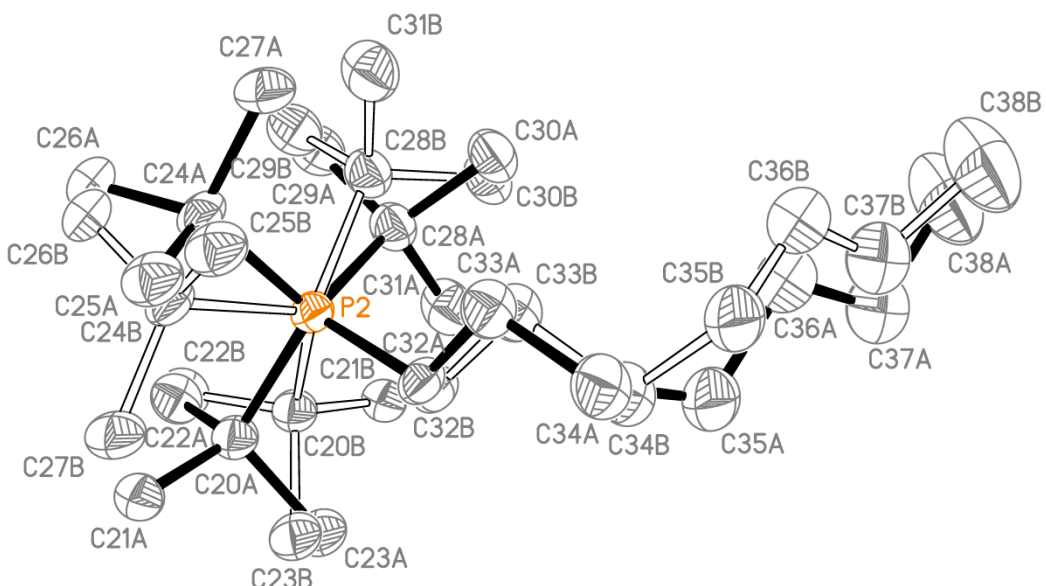


Figure S10. The second crystallographically non-equivalent cation $[{}^t\text{Bu}_3\text{P}(n\text{-C}_7\text{H}_{15})]^+$ in **4b**. Hydrogen atoms are omitted. The displacement ellipsoids are set to the 50% probability level. The A/B disorder ratio is 0.904(2): 0.096(2) for three ${}^t\text{Bu}$ fragments and 0.772(4):0.228(4) for the n-C₇H₁₅ aliphatic chain.

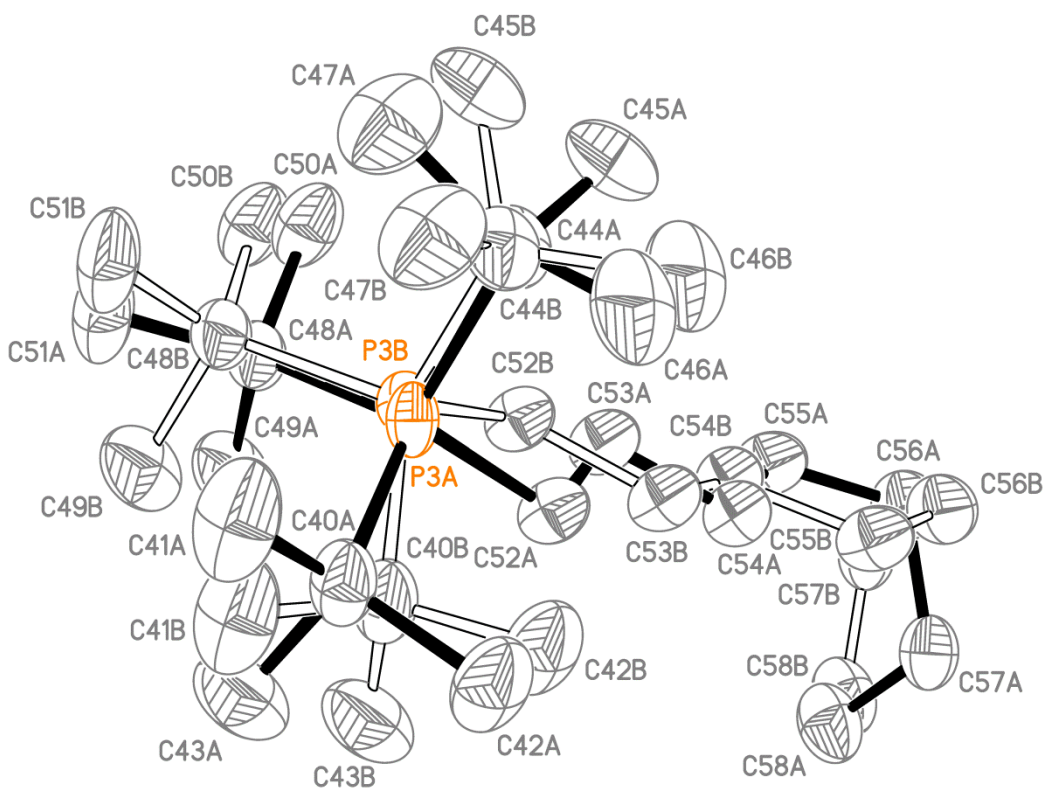


Figure S11. The third crystallographically non-equivalent cation $[{}^t\text{Bu}_3\text{P}(n\text{-C}_7\text{H}_{15})]^+$ in **4b**. Hydrogen atoms are omitted. The displacement ellipsoids are set to the 50% probability level. The A/B disorder ratio is 0.6176(16):0.3824(16).

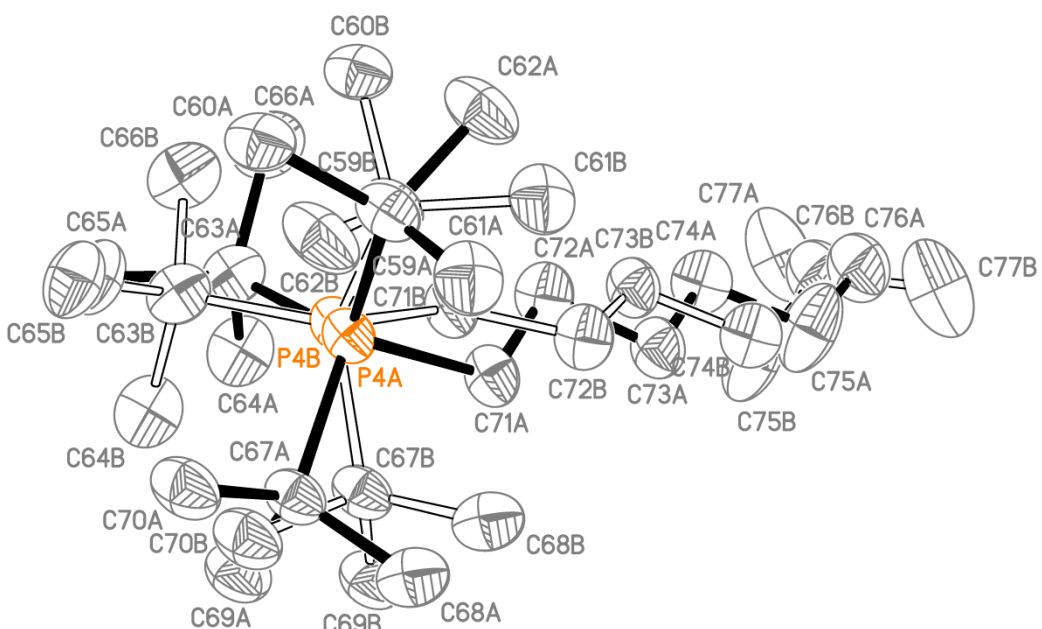


Figure S12. The fourth crystallographically non-equivalent cation $[{}^t\text{Bu}_3\text{P}(n\text{-C}_7\text{H}_{15})]^+$ in **4b**. Hydrogen atoms are omitted. The displacement ellipsoids are set to the 50% probability level. The A/B disorder ratio is 0.8810(16):0.1190(16).

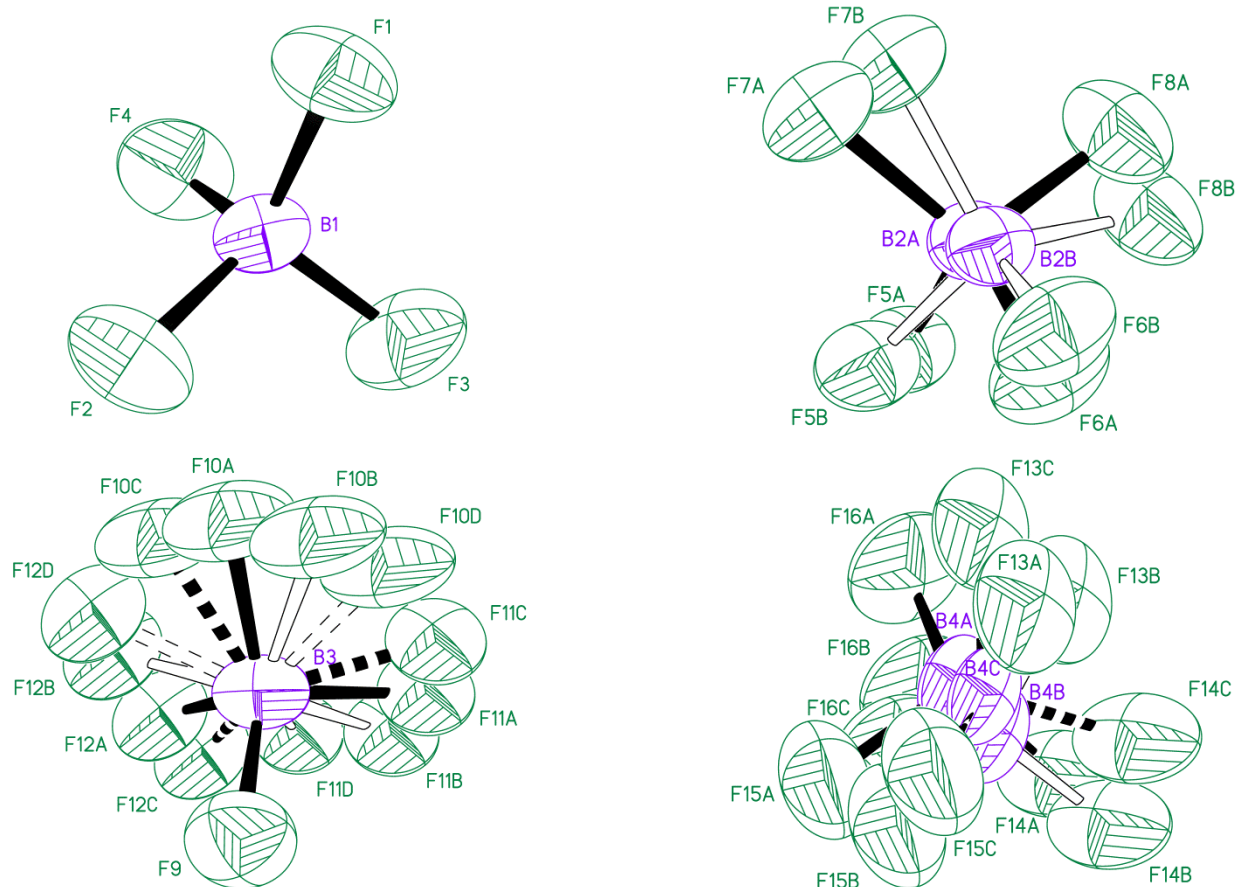


Figure S13. Four crystallographically non-equivalent anion $[\text{BF}_4]^-$ in **4b**. The displacement ellipsoids are set to the 50% probability level. The A/B disorder ratio for atoms B2, F5..F8 is 0.884(8):0.116(8). The A/B/C disorder ratio for atoms F10..F12 is 0.515(3):0.198(3):0.087(2). The A/B/C disorder ratio for atoms B4, F13..F16 is 0.753(3):0.133(3):0.114(2).

Table S8. Bond lengths for **4b** / Å.

Bond	Distance	Bond	Distance	Bond	Distance
P(1)-C(1)	1.886(2)	P(3A)-C(40A)	1.888(4)	P(4B)-C(59B)	1.887(4)
P(1)-C(5)	1.884(2)	P(3A)-C(44A)	1.887(3)	P(4B)-C(63B)	1.884(4)
P(1)-C(9)	1.887(2)	P(3A)-C(48A)	1.882(4)	P(4B)-C(67B)	1.879(4)
P(1)-C(13)	1.823(2)	P(3A)-C(52A)	1.828(4)	P(4B)-C(71B)	1.822(4)
C(1)-C(2)	1.540(3)	C(40A)-C(41A)	1.517(7)	C(59B)-C(60B)	1.530(5)
C(1)-C(3)	1.542(3)	C(40A)-C(42A)	1.539(5)	C(59B)-C(61B)	1.539(5)
C(1)-C(4)	1.546(3)	C(40A)-C(43A)	1.548(7)	C(59B)-C(62B)	1.543(5)
C(5)-C(6)	1.540(3)	C(44A)-C(45A)	1.527(6)	C(63B)-C(64B)	1.552(5)
C(5)-C(7)	1.550(3)	C(44A)-C(46A)	1.541(6)	C(63B)-C(65B)	1.552(6)
C(5)-C(8)	1.536(3)	C(44A)-C(47A)	1.531(6)	C(63B)-C(66B)	1.546(6)
C(9)-C(10)	1.542(3)	C(48A)-C(49A)	1.555(6)	C(67B)-C(68B)	1.536(5)
C(9)-C(11)	1.541(3)	C(48A)-C(50A)	1.535(5)	C(67B)-C(69B)	1.544(5)
C(9)-C(12)	1.533(3)	C(48A)-C(51A)	1.545(6)	C(67B)-C(70B)	1.543(5)
C(13)-C(14)	1.536(3)	C(52A)-C(53A)	1.529(3)	C(71B)-C(72B)	1.522(3)
C(14)-C(15)	1.529(3)	C(53A)-C(54A)	1.527(3)	C(72B)-C(73B)	1.522(3)
C(15)-C(16)	1.499(3)	C(54A)-C(55A)	1.527(3)	C(73B)-C(74B)	1.522(3)

C(16)-C(17)	1.532(4)	C(55A)-C(56A)	1.527(3)	C(74B)-C(75B)	1.522(3)
C(17)-C(18)	1.505(4)	C(56A)-C(57A)	1.524(4)	C(75B)-C(76B)	1.521(3)
C(18)-C(19)	1.526(5)	C(57A)-C(58A)	1.526(4)	C(76B)-C(77B)	1.522(3)
P(2)-C(20A)	1.890(3)	P(3B)-C(40B)	1.888(4)	F(1)-B(1)	1.379(3)
P(2)-C(24A)	1.891(3)	P(3B)-C(44B)	1.889(4)	F(2)-B(1)	1.392(3)
P(2)-C(28A)	1.878(3)	P(3B)-C(48B)	1.882(4)	F(3)-B(1)	1.377(3)
P(2)-C(20B)	1.892(4)	P(3B)-C(52B)	1.827(4)	F(4)-B(1)	1.388(3)
P(2)-C(24B)	1.889(4)	C(40B)-C(41B)	1.516(7)	F(5A)-B(2A)	1.3927(19)
P(2)-C(28B)	1.878(4)	C(40B)-C(42B)	1.540(5)	F(6A)-B(2A)	1.3902(19)
P(2)-C(32A)	1.836(2)	C(40B)-C(43B)	1.548(7)	F(7A)-B(2A)	1.3891(19)
P(2)-C(32B)	1.836(3)	C(44B)-C(45B)	1.528(6)	F(8A)-B(2A)	1.388(2)
C(20A)-C(21A)	1.543(4)	C(44B)-C(46B)	1.542(6)	F(5B)-B(2B)	1.390(3)
C(20A)-C(22A)	1.540(5)	C(44B)-C(47B)	1.532(6)	F(6B)-B(2B)	1.389(3)
C(20A)-C(23A)	1.553(4)	C(48B)-C(49B)	1.555(6)	F(7B)-B(2B)	1.389(3)
C(24A)-C(25A)	1.546(4)	C(48B)-C(50B)	1.536(5)	F(8B)-B(2B)	1.389(3)
C(24A)-C(26A)	1.533(4)	C(48B)-C(51B)	1.545(6)	F(9)-B(3)	1.381(4)
C(24A)-C(27A)	1.542(4)	C(52B)-C(53B)	1.526(4)	F(10A)-B(3)	1.391(2)
C(28A)-C(29A)	1.536(4)	C(53B)-C(54B)	1.526(4)	F(11A)-B(3)	1.400(2)
C(28A)-C(30A)	1.553(4)	C(54B)-C(55B)	1.525(4)	F(12A)-B(3)	1.401(2)
C(28A)-C(31A)	1.534(4)	C(55B)-C(56B)	1.525(4)	F(10B)-B(3)	1.397(3)
C(20B)-C(21B)	1.543(5)	C(56B)-C(57B)	1.523(4)	F(11B)-B(3)	1.394(3)
C(20B)-C(22B)	1.540(5)	C(57B)-C(58B)	1.525(4)	F(12B)-B(3)	1.395(3)
C(20B)-C(23B)	1.553(5)	P(4A)-C(59A)	1.887(3)	F(10C)-B(3)	1.395(3)
C(24B)-C(25B)	1.546(5)	P(4A)-C(63A)	1.885(3)	F(11C)-B(3)	1.396(3)
C(24B)-C(26B)	1.533(5)	P(4A)-C(67A)	1.878(3)	F(12C)-B(3)	1.396(3)
C(24B)-C(27B)	1.542(5)	P(4A)-C(71A)	1.824(3)	F(10D)-B(3)	1.396(3)
C(28B)-C(29B)	1.537(5)	C(59A)-C(60A)	1.529(4)	F(11D)-B(3)	1.393(3)
C(28B)-C(30B)	1.553(5)	C(59A)-C(61A)	1.539(4)	F(12D)-B(3)	1.397(3)
C(28B)-C(31B)	1.534(5)	C(59A)-C(62A)	1.543(4)	F(13A)-B(4A)	1.367(2)
C(32A)-C(33A)	1.525(2)	C(63A)-C(64A)	1.551(4)	F(14A)-B(4A)	1.368(2)
C(33A)-C(34A)	1.521(2)	C(63A)-C(65A)	1.552(5)	F(15A)-B(4A)	1.368(2)
C(34A)-C(35A)	1.516(3)	C(63A)-C(66A)	1.545(5)	F(16A)-B(4A)	1.368(2)
C(35A)-C(36A)	1.517(3)	C(67A)-C(68A)	1.536(4)	F(13B)-B(4B)	1.367(3)
C(36A)-C(37A)	1.514(3)	C(67A)-C(69A)	1.543(4)	F(14B)-B(4B)	1.367(3)
C(37A)-C(38A)	1.516(3)	C(67A)-C(70A)	1.543(4)	F(15B)-B(4B)	1.367(3)
C(32B)-C(33B)	1.519(3)	C(71A)-C(72A)	1.523(2)	F(16B)-B(4B)	1.368(3)
C(33B)-C(34B)	1.519(3)	C(72A)-C(73A)	1.522(2)	F(13C)-B(4C)	1.367(3)
C(34B)-C(35B)	1.518(3)	C(73A)-C(74A)	1.524(2)	F(14C)-B(4C)	1.367(3)
C(35B)-C(36B)	1.518(3)	C(74A)-C(75A)	1.522(3)	F(15C)-B(4C)	1.367(3)
C(36B)-C(37B)	1.518(3)	C(75A)-C(76A)	1.517(3)	F(16C)-B(4C)	1.367(3)
C(37B)-C(38B)	1.518(3)	C(76A)-C(77A)	1.520(3)		

Table S9. Bond angles for **4b** / °.

Bond angle	Value	Bond angle	Value
C(1)-P(1)-C(9)	111.69(10)	C(45B)-C(44B)-P(3B)	110.0(5)
C(5)-P(1)-C(1)	111.27(10)	C(45B)-C(44B)-C(46B)	106.5(8)
C(5)-P(1)-C(9)	112.00(10)	C(45B)-C(44B)-C(47B)	107.8(7)
C(13)-P(1)-C(1)	103.75(10)	C(46B)-C(44B)-P(3B)	111.0(6)
C(13)-P(1)-C(5)	110.05(10)	C(47B)-C(44B)-P(3B)	113.0(6)
C(13)-P(1)-C(9)	107.69(11)	C(47B)-C(44B)-C(46B)	108.3(7)
C(2)-C(1)-P(1)	112.54(15)	C(49B)-C(48B)-P(3B)	108.7(7)
C(2)-C(1)-C(3)	107.94(19)	C(50B)-C(48B)-P(3B)	110.6(7)
C(2)-C(1)-C(4)	108.70(19)	C(50B)-C(48B)-C(49B)	108.7(10)
C(3)-C(1)-P(1)	110.96(15)	C(50B)-C(48B)-C(51B)	109.8(10)
C(3)-C(1)-C(4)	105.47(19)	C(51B)-C(48B)-P(3B)	111.3(8)
C(4)-C(1)-P(1)	110.93(16)	C(51B)-C(48B)-C(49B)	107.6(9)
C(6)-C(5)-P(1)	112.37(15)	C(53B)-C(52B)-P(3B)	121.0(5)
C(6)-C(5)-C(7)	108.22(18)	C(54B)-C(53B)-C(52B)	110.9(5)
C(7)-C(5)-P(1)	110.43(14)	C(55B)-C(54B)-C(53B)	111.1(7)
C(8)-C(5)-P(1)	110.91(15)	C(56B)-C(55B)-C(54B)	115.0(7)
C(8)-C(5)-C(6)	108.12(17)	C(57B)-C(56B)-C(55B)	115.3(7)
C(8)-C(5)-C(7)	106.57(18)	C(56B)-C(57B)-C(58B)	110.3(10)
C(10)-C(9)-P(1)	110.79(16)	C(63A)-P(4A)-C(59A)	112.36(15)
C(11)-C(9)-P(1)	110.07(16)	C(67A)-P(4A)-C(59A)	111.62(13)
C(11)-C(9)-C(10)	105.1(2)	C(67A)-P(4A)-C(63A)	110.99(16)
C(12)-C(9)-P(1)	112.31(16)	C(71A)-P(4A)-C(59A)	108.40(15)
C(12)-C(9)-C(10)	109.32(19)	C(71A)-P(4A)-C(63A)	110.70(14)
C(12)-C(9)-C(11)	109.02(19)	C(71A)-P(4A)-C(67A)	102.28(14)
C(14)-C(13)-P(1)	122.42(16)	C(60A)-C(59A)-P(4A)	112.4(2)
C(15)-C(14)-C(13)	108.5(2)	C(60A)-C(59A)-C(61A)	109.0(2)
C(16)-C(15)-C(14)	114.8(2)	C(60A)-C(59A)-C(62A)	110.0(3)
C(15)-C(16)-C(17)	112.3(2)	C(61A)-C(59A)-P(4A)	110.6(2)
C(18)-C(17)-C(16)	115.0(3)	C(61A)-C(59A)-C(62A)	104.8(3)
C(17)-C(18)-C(19)	111.6(3)	C(62A)-C(59A)-P(4A)	109.8(2)
C(20A)-P(2)-C(24A)	110.81(12)	C(64A)-C(63A)-P(4A)	110.4(2)
C(28A)-P(2)-C(20A)	111.98(12)	C(64A)-C(63A)-C(65A)	107.9(3)
C(28A)-P(2)-C(24A)	111.94(12)	C(65A)-C(63A)-P(4A)	112.3(2)
C(24B)-P(2)-C(20B)	113.1(8)	C(66A)-C(63A)-P(4A)	109.4(3)
C(28B)-P(2)-C(20B)	106.6(8)	C(66A)-C(63A)-C(64A)	107.6(3)
C(28B)-P(2)-C(24B)	116.6(8)	C(66A)-C(63A)-C(65A)	109.2(3)
C(32A)-P(2)-C(20A)	105.50(17)	C(68A)-C(67A)-P(4A)	110.9(2)

C(32A)-P(2)-C(24A)	107.27(15)	C(68A)-C(67A)-C(69A)	106.8(3)
C(32A)-P(2)-C(28A)	109.0(2)	C(68A)-C(67A)-C(70A)	108.6(3)
C(32B)-P(2)-C(20B)	100.2(8)	C(69A)-C(67A)-P(4A)	110.3(2)
C(32B)-P(2)-C(24B)	109.7(10)	C(69A)-C(67A)-C(70A)	107.5(3)
C(32B)-P(2)-C(28B)	109.4(10)	C(70A)-C(67A)-P(4A)	112.5(2)
C(21A)-C(20A)-P(2)	110.82(18)	C(72A)-C(71A)-P(4A)	122.6(2)
C(21A)-C(20A)-C(23A)	105.6(2)	C(75A)-C(74A)-C(73A)	113.0(3)
C(22A)-C(20A)-P(2)	112.4(4)	C(63B)-P(4B)-C(59B)	115.8(9)
C(22A)-C(20A)-C(21A)	107.8(3)	C(67B)-P(4B)-C(59B)	108.7(8)
C(22A)-C(20A)-C(23A)	109.5(4)	C(67B)-P(4B)-C(63B)	114.4(9)
C(23A)-C(20A)-P(2)	110.6(2)	C(71B)-P(4B)-C(59B)	103.5(10)
C(25A)-C(24A)-P(2)	111.04(18)	C(71B)-P(4B)-C(63B)	110.8(10)
C(26A)-C(24A)-P(2)	113.0(2)	C(71B)-P(4B)-C(67B)	102.2(10)
C(26A)-C(24A)-C(25A)	108.0(2)	C(60B)-C(59B)-P(4B)	107.0(12)
C(26A)-C(24A)-C(27A)	107.5(2)	C(60B)-C(59B)-C(61B)	102.5(17)
C(27A)-C(24A)-P(2)	109.61(19)	C(60B)-C(59B)-C(62B)	112.4(18)
C(27A)-C(24A)-C(25A)	107.5(2)	C(61B)-C(59B)-P(4B)	115.6(13)
C(29A)-C(28A)-P(2)	113.0(2)	C(61B)-C(59B)-C(62B)	109.6(17)
C(29A)-C(28A)-C(30A)	109.3(3)	C(62B)-C(59B)-P(4B)	109.6(13)
C(30A)-C(28A)-P(2)	111.1(2)	C(64B)-C(63B)-P(4B)	105.2(13)
C(31A)-C(28A)-P(2)	109.0(2)	C(64B)-C(63B)-C(65B)	106.4(18)
C(31A)-C(28A)-C(29A)	108.8(3)	C(65B)-C(63B)-P(4B)	108.8(13)
C(31A)-C(28A)-C(30A)	105.4(2)	C(66B)-C(63B)-P(4B)	109.5(15)
C(21B)-C(20B)-P(2)	115.6(13)	C(66B)-C(63B)-C(64B)	118.0(19)
C(21B)-C(20B)-C(23B)	107.2(18)	C(66B)-C(63B)-C(65B)	108.6(18)
C(22B)-C(20B)-P(2)	112(4)	C(68B)-C(67B)-P(4B)	116.2(13)
C(22B)-C(20B)-C(21B)	107(2)	C(68B)-C(67B)-C(69B)	103.2(17)
C(22B)-C(20B)-C(23B)	107(2)	C(68B)-C(67B)-C(70B)	105.0(17)
C(23B)-C(20B)-P(2)	107(3)	C(69B)-C(67B)-P(4B)	113.4(14)
C(25B)-C(24B)-P(2)	103.3(13)	C(70B)-C(67B)-P(4B)	109.0(13)
C(26B)-C(24B)-P(2)	106(2)	C(70B)-C(67B)-C(69B)	109.5(17)
C(26B)-C(24B)-C(25B)	113.8(14)	C(72B)-C(71B)-P(4B)	132.4(12)
C(26B)-C(24B)-C(27B)	113.5(13)	C(73B)-C(72B)-C(71B)	111.9(10)
C(27B)-C(24B)-P(2)	107.8(13)	C(72B)-C(73B)-C(74B)	111.2(11)
C(27B)-C(24B)-C(25B)	111.7(12)	C(75B)-C(74B)-C(73B)	108.3(11)
C(29B)-C(28B)-P(2)	114(2)	C(76B)-C(75B)-C(74B)	112.4(14)
C(29B)-C(28B)-C(30B)	104.7(15)	C(75B)-C(76B)-C(77B)	110.9(13)
C(30B)-C(28B)-P(2)	116.7(15)	F(1)-B(1)-F(2)	110.5(2)
C(31B)-C(28B)-P(2)	109.9(15)	F(1)-B(1)-F(4)	110.4(2)
C(31B)-C(28B)-C(29B)	104.6(14)	F(3)-B(1)-F(1)	109.9(2)
C(31B)-C(28B)-C(30B)	106.0(13)	F(3)-B(1)-F(2)	108.0(2)

C(33A)-C(32A)-P(2)	123.4(3)	F(3)-B(1)-F(4)	108.0(2)
C(34A)-C(33A)-C(32A)	112.5(3)	F(4)-B(1)-F(2)	109.9(2)
C(35A)-C(34A)-C(33A)	114.7(3)	F(6A)-B(2A)-F(5A)	109.7(2)
C(34A)-C(35A)-C(36A)	115.1(3)	F(7A)-B(2A)-F(5A)	110.1(2)
C(37A)-C(36A)-C(35A)	109.3(4)	F(7A)-B(2A)-F(6A)	109.8(2)
C(36A)-C(37A)-C(38A)	113.3(5)	F(8A)-B(2A)-F(5A)	108.5(2)
C(33B)-C(32B)-P(2)	116.5(8)	F(8A)-B(2A)-F(6A)	109.6(2)
C(34B)-C(33B)-C(32B)	109.1(8)	F(8A)-B(2A)-F(7A)	109.2(2)
C(35B)-C(34B)-C(33B)	114.0(11)	F(6B)-B(2B)-F(5B)	111.5(12)
C(35B)-C(36B)-C(37B)	123.6(14)	F(6B)-B(2B)-F(8B)	108.7(12)
C(38B)-C(37B)-C(36B)	106.2(12)	F(7B)-B(2B)-F(5B)	107.6(12)
C(44A)-P(3A)-C(40A)	112.0(3)	F(7B)-B(2B)-F(6B)	109.2(12)
C(48A)-P(3A)-C(40A)	111.7(4)	F(7B)-B(2B)-F(8B)	108.6(11)
C(48A)-P(3A)-C(44A)	112.1(3)	F(8B)-B(2B)-F(5B)	111.2(12)
C(52A)-P(3A)-C(40A)	104.5(2)	F(9)-B(3)-F(10A)	109.8(3)
C(52A)-P(3A)-C(44A)	107.3(3)	F(9)-B(3)-F(11A)	109.9(3)
C(52A)-P(3A)-C(48A)	108.7(3)	F(9)-B(3)-F(10B)	104.1(7)
C(41A)-C(40A)-P(3A)	112.7(4)	F(9)-B(3)-F(11B)	107.5(8)
C(41A)-C(40A)-C(42A)	109.6(5)	F(9)-B(3)-F(12B)	113.2(5)
C(41A)-C(40A)-C(43A)	108.8(5)	F(9)-B(3)-F(10C)	113.2(8)
C(42A)-C(40A)-P(3A)	110.7(4)	F(9)-B(3)-F(11C)	111.9(7)
C(42A)-C(40A)-C(43A)	106.6(5)	F(9)-B(3)-F(12C)	105.0(9)
C(43A)-C(40A)-P(3A)	108.2(4)	F(9)-B(3)-F(10D)	106.3(10)
C(45A)-C(44A)-P(3A)	112.1(4)	F(9)-B(3)-F(11D)	117.5(8)
C(45A)-C(44A)-C(46A)	106.4(5)	F(9)-B(3)-F(12D)	102.4(10)
C(45A)-C(44A)-C(47A)	107.7(5)	F(10A)-B(3)-F(11A)	109.1(3)
C(46A)-C(44A)-P(3A)	109.6(4)	F(11B)-B(3)-F(10B)	108.2(7)
C(47A)-C(44A)-P(3A)	111.8(4)	F(11B)-B(3)-F(12B)	113.7(8)
C(47A)-C(44A)-C(46A)	109.1(5)	F(12B)-B(3)-F(10B)	109.6(7)
C(49A)-C(48A)-P(3A)	110.2(4)	F(10C)-B(3)-F(11C)	108.4(8)
C(50A)-C(48A)-P(3A)	110.4(4)	F(10C)-B(3)-F(12C)	107.7(8)
C(50A)-C(48A)-C(49A)	103.5(6)	F(11C)-B(3)-F(12C)	110.5(9)
C(50A)-C(48A)-C(51A)	108.4(5)	F(10D)-B(3)-F(12D)	108.5(11)
C(51A)-C(48A)-P(3A)	113.0(5)	F(11D)-B(3)-F(10D)	113.3(11)
C(51A)-C(48A)-C(49A)	111.1(5)	F(11D)-B(3)-F(12D)	108.1(11)
C(53A)-C(52A)-P(3A)	123.0(3)	F(13A)-B(4A)-F(14A)	112.1(3)
C(54A)-C(53A)-C(52A)	109.9(3)	F(13A)-B(4A)-F(15A)	108.9(3)
C(55A)-C(54A)-C(53A)	111.5(4)	F(13A)-B(4A)-F(16A)	105.7(3)
C(54A)-C(55A)-C(56A)	113.6(4)	F(14A)-B(4A)-F(16A)	111.4(3)
C(57A)-C(56A)-C(55A)	114.2(4)	F(15A)-B(4A)-F(14A)	108.5(3)
C(56A)-C(57A)-C(58A)	114.5(6)	F(15A)-B(4A)-F(16A)	110.3(3)

C(40B)-P(3B)-C(44B)	111.6(5)	F(14B)-B(4B)-F(13B)	108.0(12)
C(48B)-P(3B)-C(40B)	112.1(6)	F(14B)-B(4B)-F(16B)	105.5(12)
C(48B)-P(3B)-C(44B)	111.3(4)	F(15B)-B(4B)-F(13B)	109.6(12)
C(52B)-P(3B)-C(40B)	111.0(4)	F(15B)-B(4B)-F(14B)	109.5(12)
C(52B)-P(3B)-C(44B)	107.1(5)	F(15B)-B(4B)-F(16B)	113.6(12)
C(52B)-P(3B)-C(48B)	103.3(5)	F(16B)-B(4B)-F(13B)	110.5(12)
C(41B)-C(40B)-P(3B)	112.5(6)	F(14C)-B(4C)-F(13C)	107.0(11)
C(41B)-C(40B)-C(42B)	109.6(7)	F(14C)-B(4C)-F(15C)	108.6(11)
C(41B)-C(40B)-C(43B)	108.6(8)	F(14C)-B(4C)-F(16C)	110.3(12)
C(42B)-C(40B)-P(3B)	110.4(6)	F(15C)-B(4C)-F(13C)	113.4(12)
C(42B)-C(40B)-C(43B)	105.9(8)	F(16C)-B(4C)-F(13C)	110.4(12)
C(43B)-C(40B)-P(3B)	109.6(6)	F(16C)-B(4C)-F(15C)	107.1(12)

Typical procedure for PdNPs preparation

0.0004 g (0.00178 mmol) of palladium acetate and 0.178 mmol of phosphonium salt (see Table S10) was dissolved in 9 mL ethanol and stirred during 20 minutes at room temperature. The color of solution changes from transparent to light brownish grey.

Table S10. The mass of PIL used in the procedure of catalyst preparation.

PIL	m, g
1b	0.054
2b	0.059
3b	0.064
4b	0.069
5b	0.074
6b	0.079
7b	0.084
8b	0.089
9b	0.094

TEM data

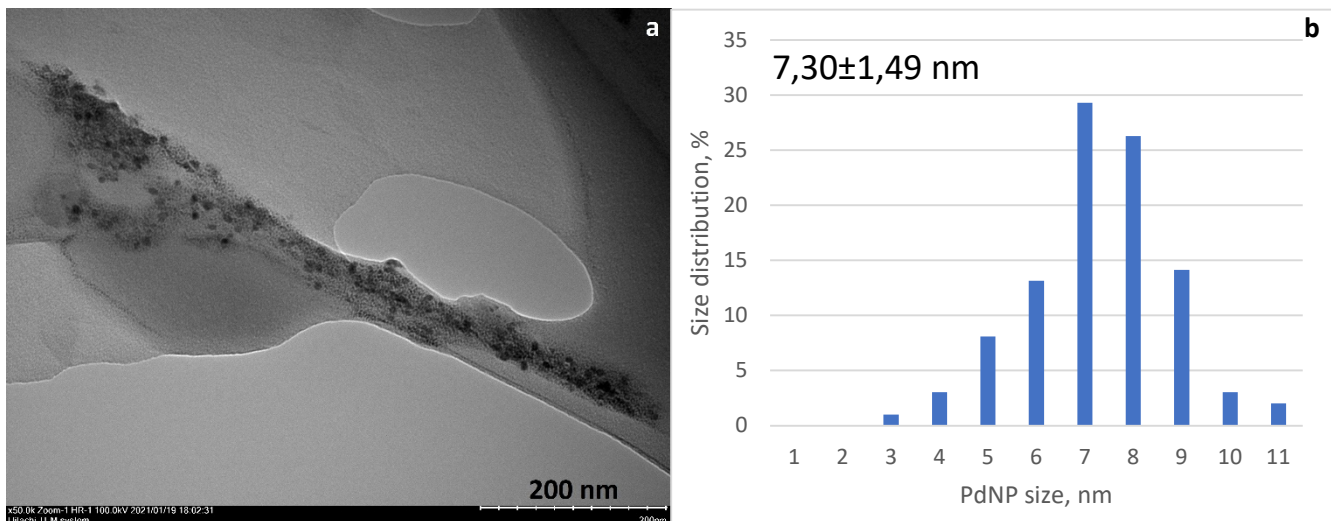


Figure S14. TEM image (a) and size distribution (b) of PdNPs in **1b** before the Suzuki reaction.

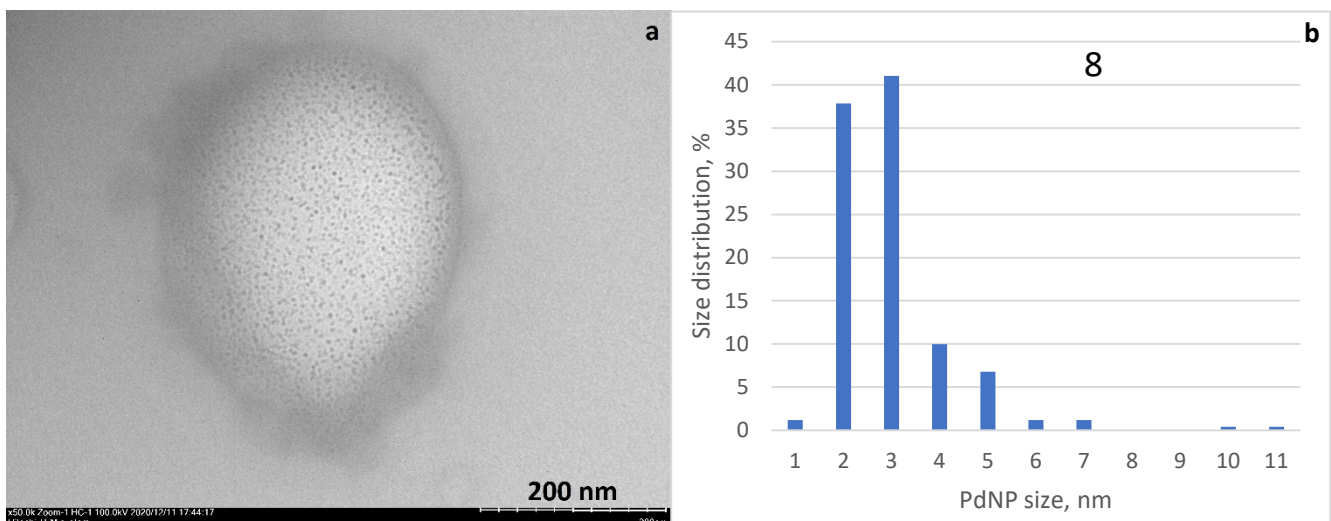


Figure S15. TEM image (a) and size distribution (b) of PdNPs in **1b** after the Suzuki reaction.

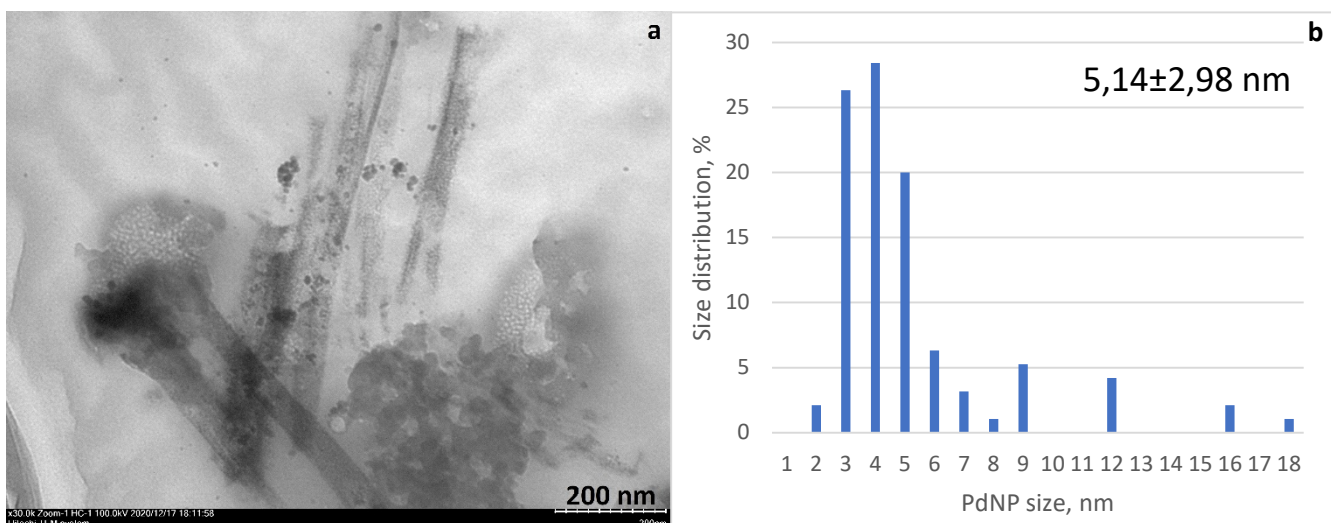


Figure S16. TEM image (a) and size distribution (b) of PdNPs in **2b** before the Suzuki reaction.

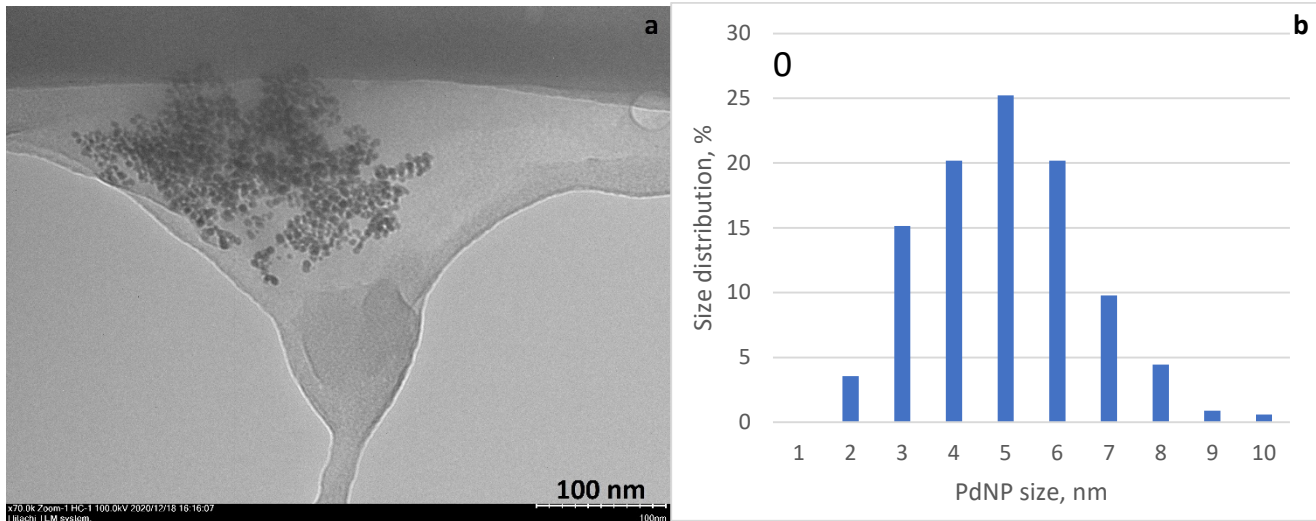


Figure S17. TEM image (a) and size distribution (b) of PdNPs in **2b** after the Suzuki reaction.

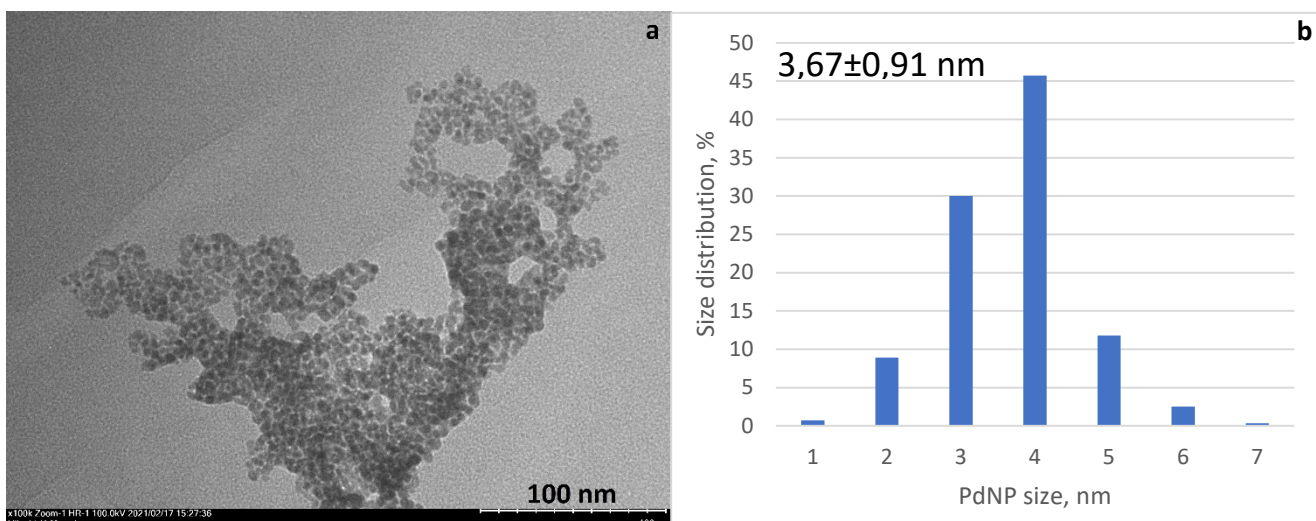


Figure S18. TEM image (a) and size distribution (b) of PdNPs in **3b** before the Suzuki reaction.

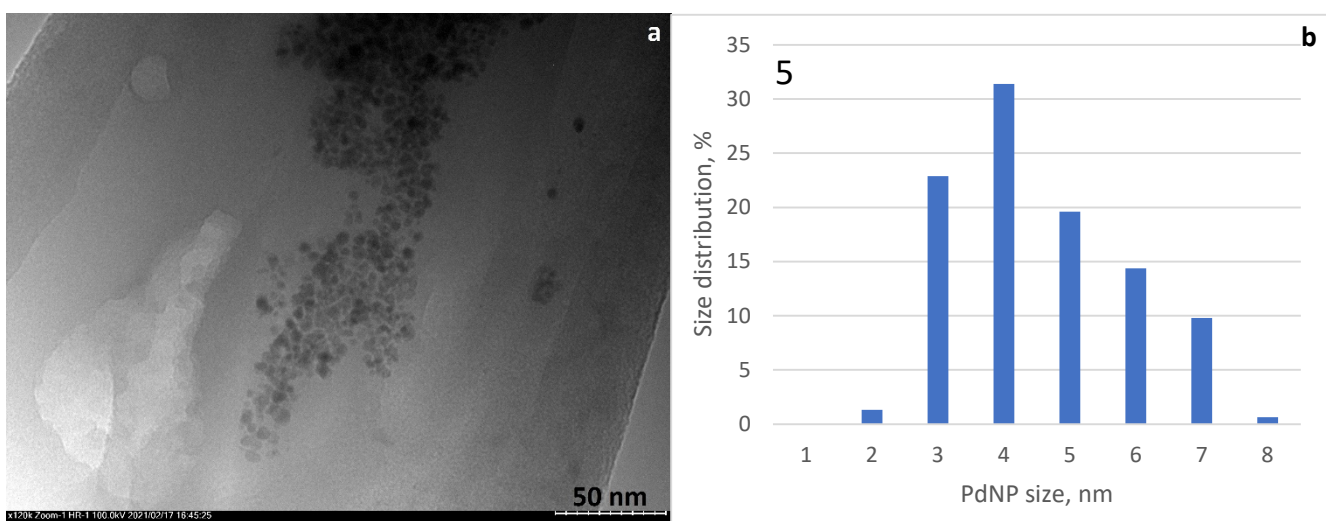


Figure S19. TEM image (a) and size distribution (b) of PdNPs in **3b** after the Suzuki reaction.

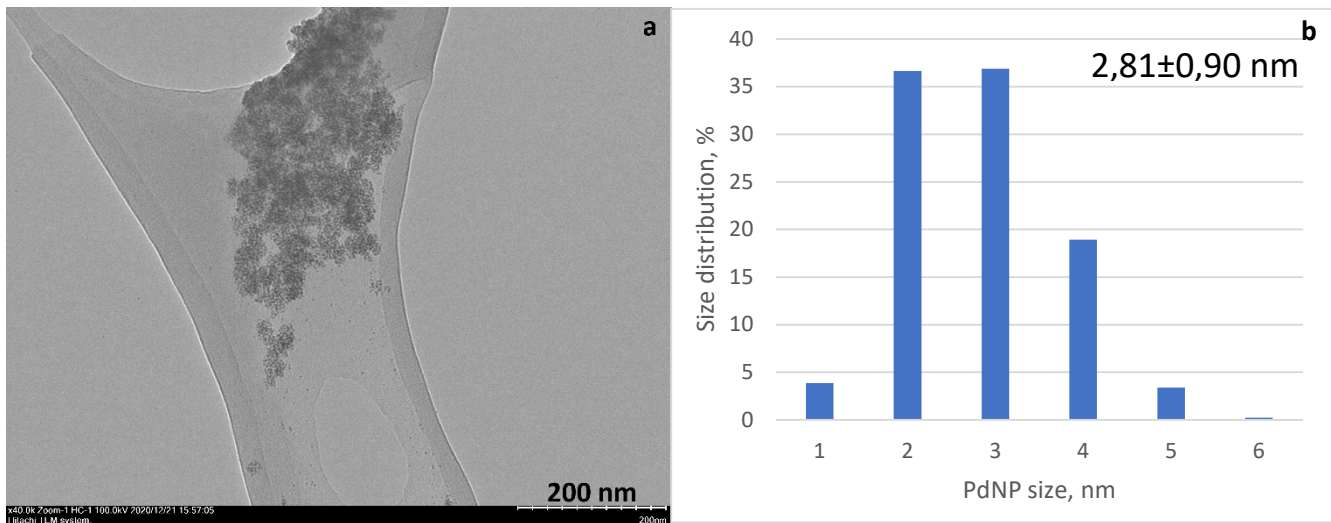


Figure S20. TEM image (a) and size distribution (b) of PdNPs in **4b** before the Suzuki reaction.

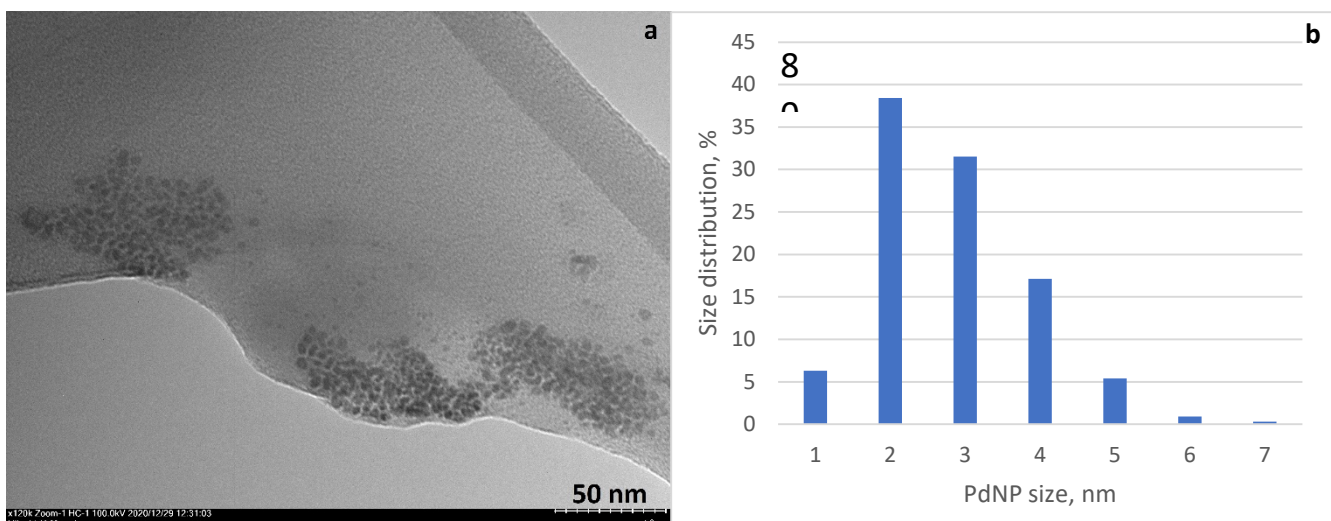


Figure S21. TEM image (a) and size distribution (b) of PdNPs in **4b** after the Suzuki reaction.

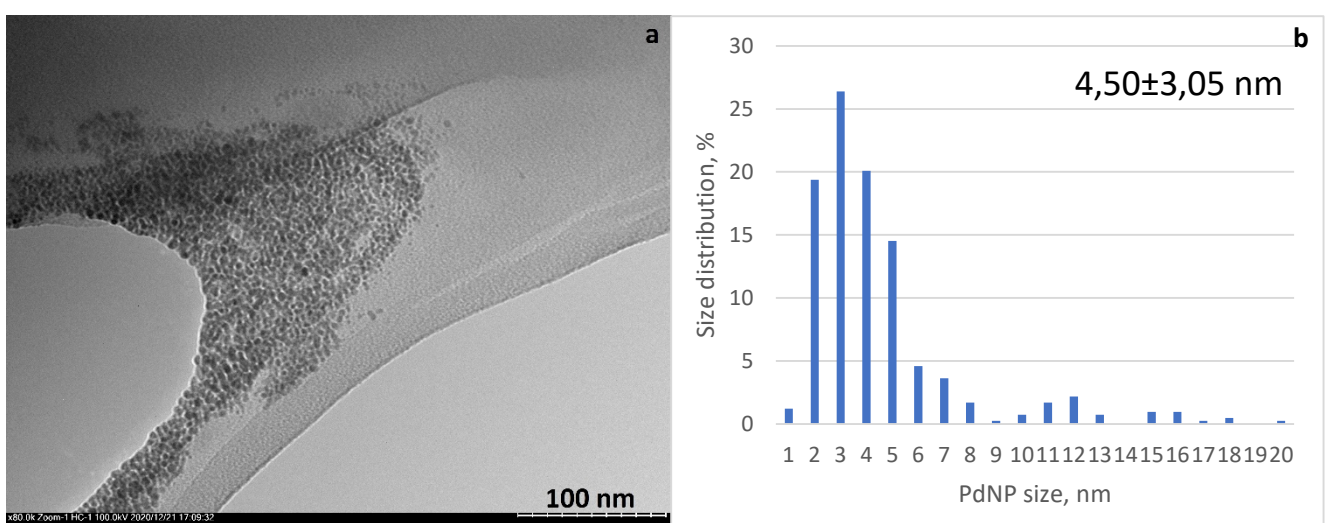


Figure S22. TEM image (a) and size distribution (b) of PdNPs in **5b** before the Suzuki reaction.

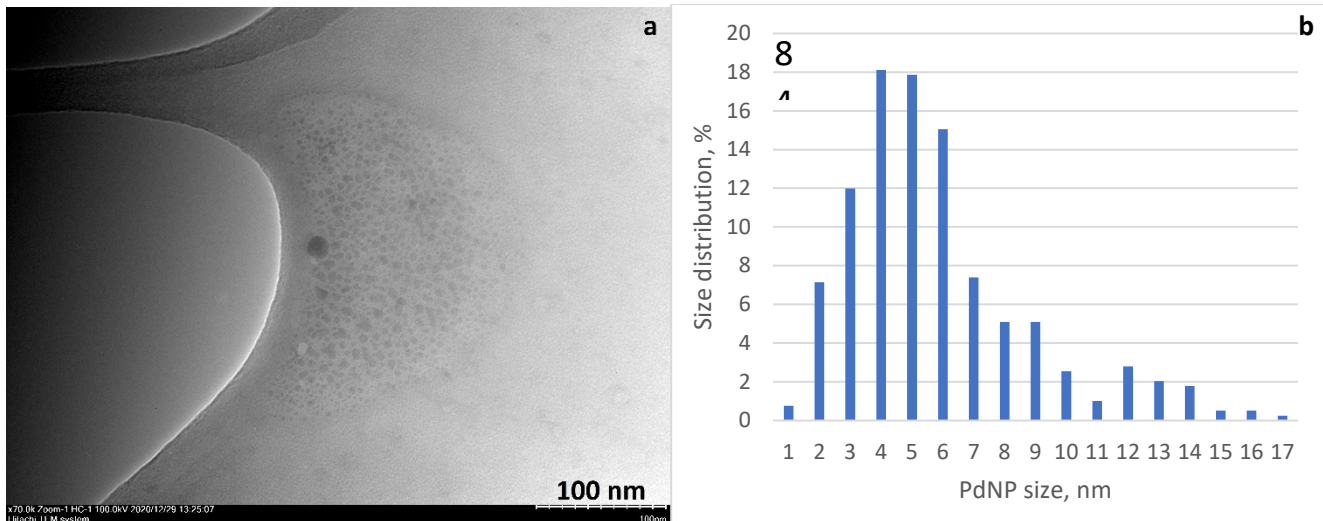


Figure S23. TEM image (a) and size distribution (b) of PdNPs in **5b** after the Suzuki reaction.

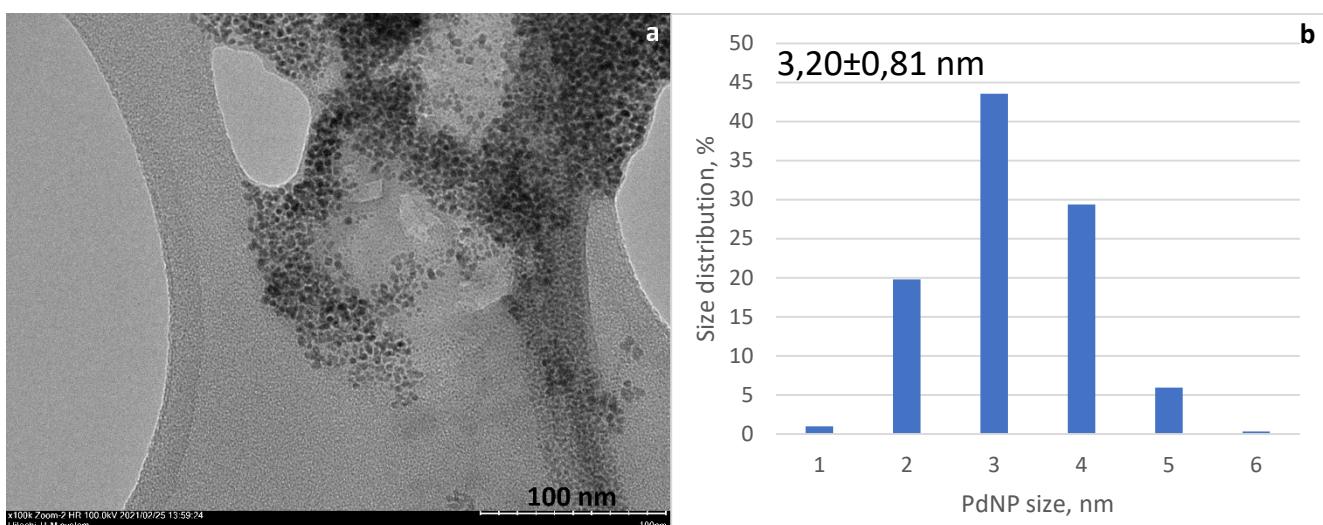


Figure S24. TEM image (a) and size distribution (b) of PdNPs in **6b** before the Suzuki reaction.

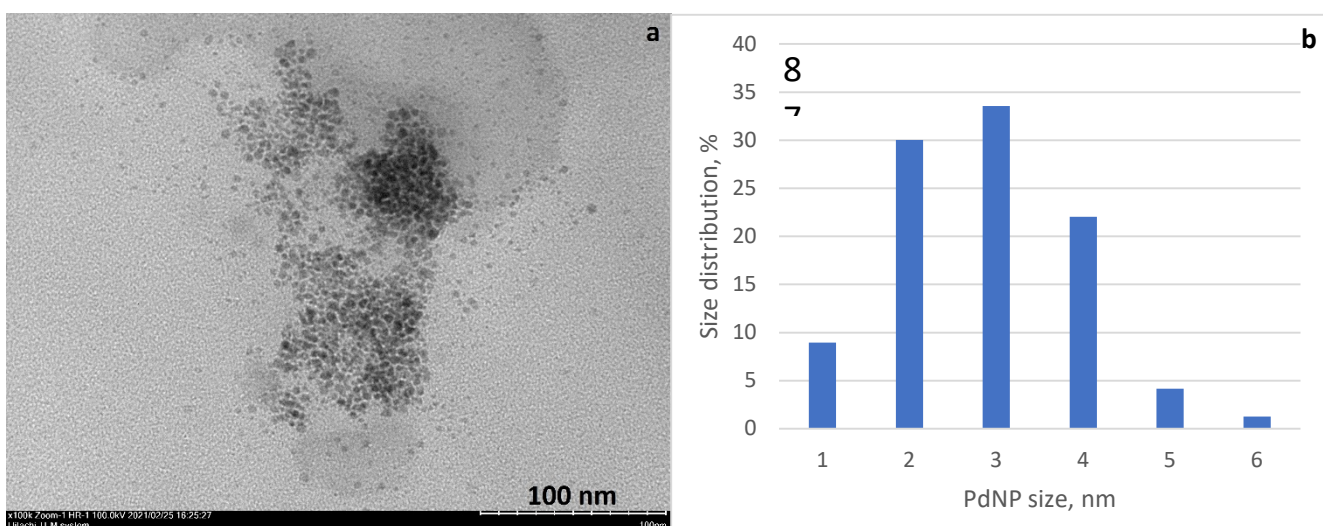


Figure S25. TEM image (a) and size distribution (b) of PdNPs in **6b** after the Suzuki reaction.

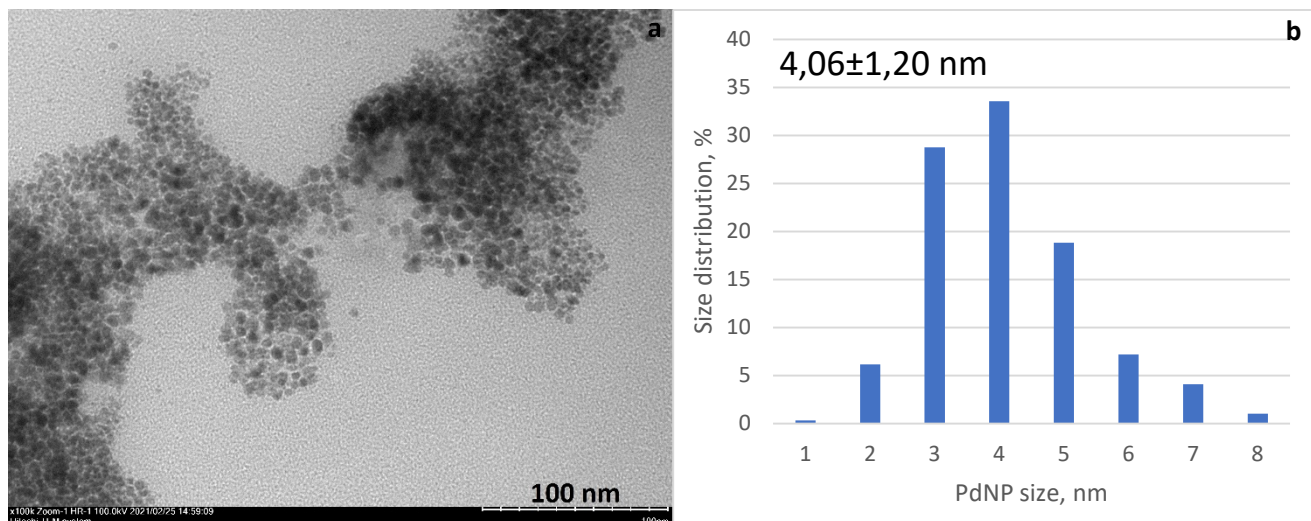


Figure S26. TEM image (a) and size distribution (b) of PdNPs in **7b** before the Suzuki reaction.

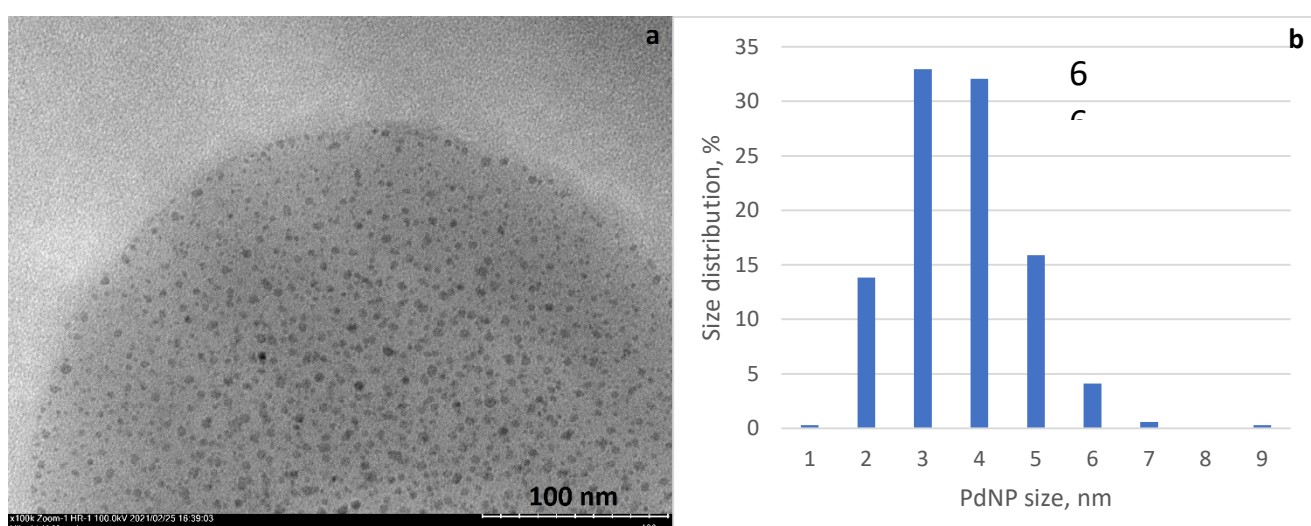


Figure S27. TEM image (a) and size distribution (b) of PdNPs in **7b** after the Suzuki reaction.

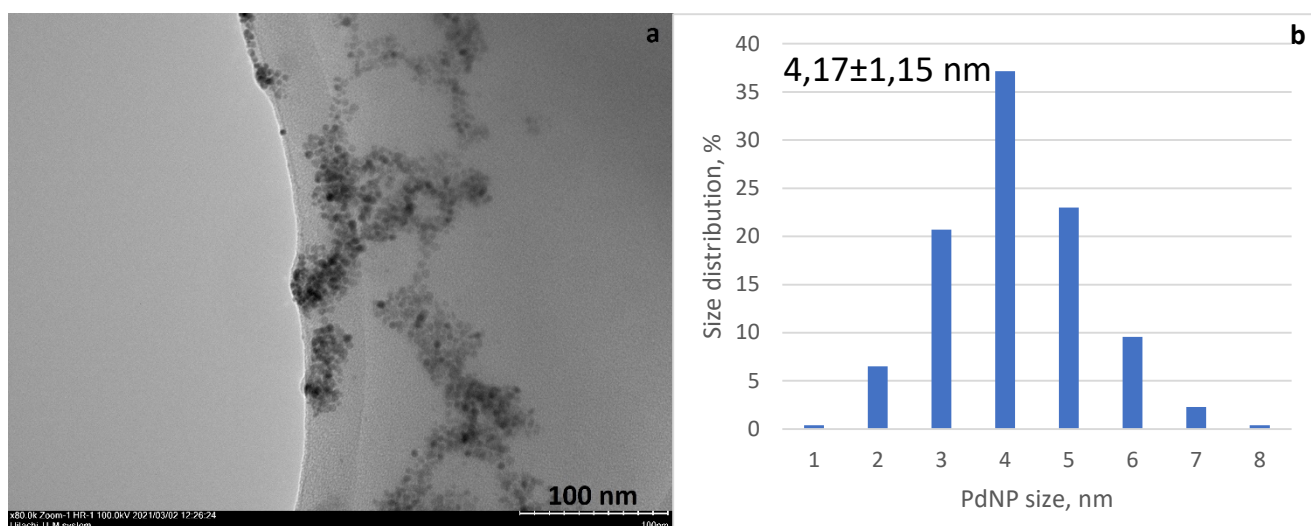


Figure S28. TEM image (a) and size distribution (b) of PdNPs in **8b** before the Suzuki reaction.

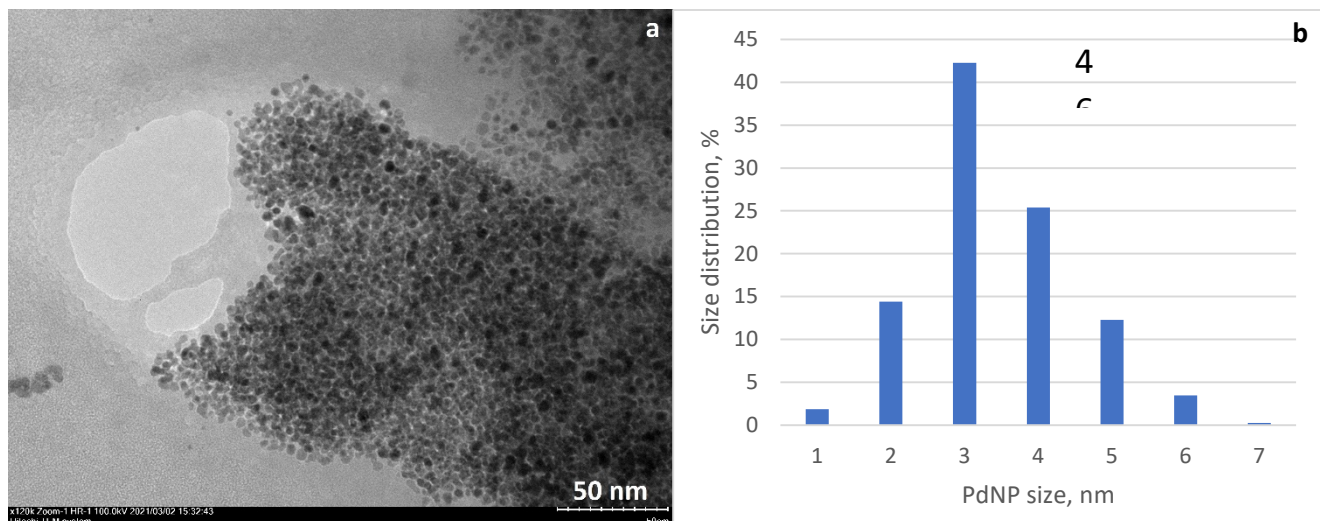


Figure S29. TEM image (a) and size distribution (b) of PdNPs in **8b** after the Suzuki reaction.

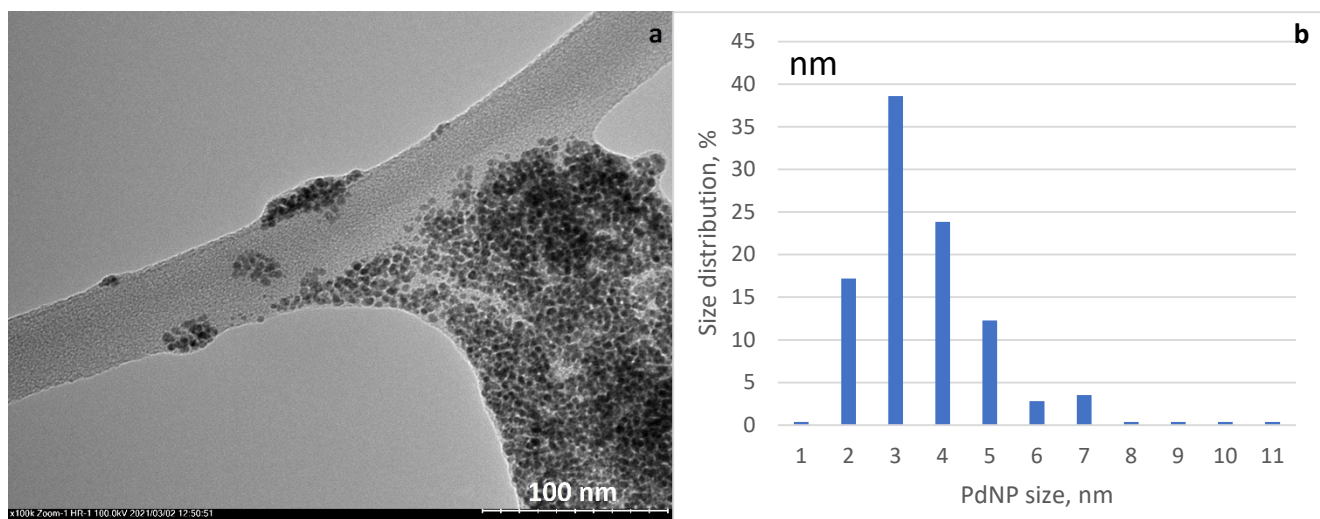


Figure S30. TEM image (a) and size distribution (b) of PdNPs in **9b** before the Suzuki reaction.

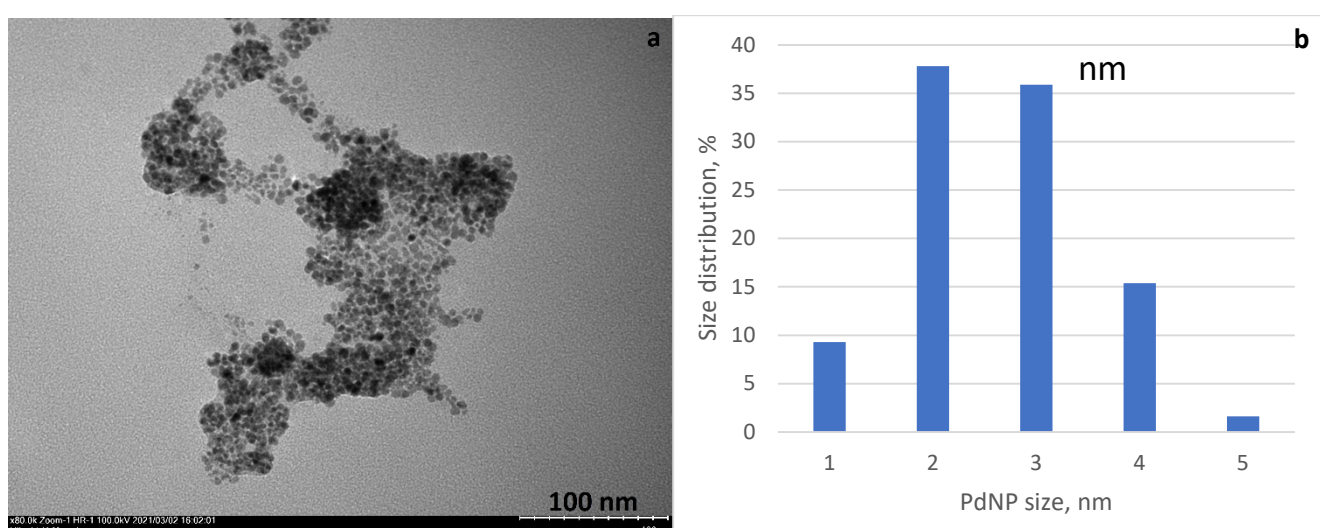


Figure S31. TEM image (a) and size distribution (b) of PdNPs in **9b** after the Suzuki reaction.

DLS data

		Diam. (nm)	% Number	Width (nm)
Z-Average (d.nm):	1926	Peak 1:	1755	2,5
Pdl:	0,470	Peak 2:	308,5	97,5
Intercept:	0,906	Peak 3:	0,000	0,000

Result quality : Refer to quality report

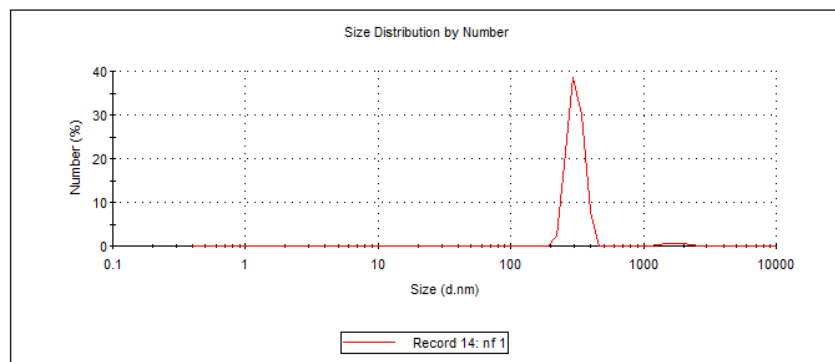


Figure S32. The size distribution of metal-organic aggregates in solution of catalytic system based on **4b**.

		Diam. (nm)	% Number	Width (nm)
Z-Average (d.nm):	1290	Peak 1:	1370	3,1
Pdl:	0,421	Peak 2:	370,5	96,9
Intercept:	0,916	Peak 3:	0,000	0,000

Result quality : Good

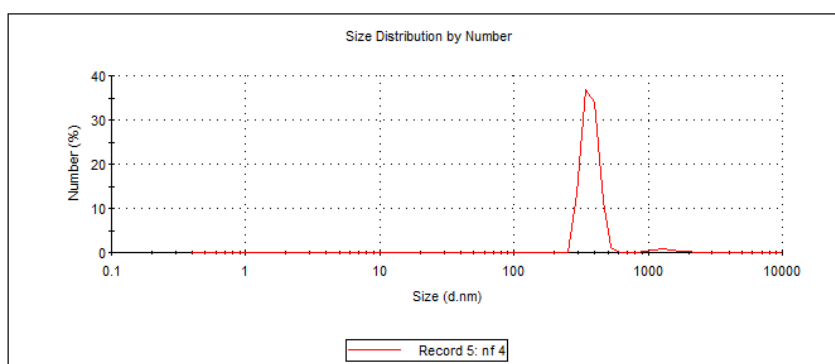


Figure S33. The size distribution of metal-organic aggregates in solution of catalytic system based on **5b**.

	Diam. (nm)	% Number	Width (nm)
Z-Average (d.nm):	667,3	32,1	144,0
Pdl:	0,370	67,9	41,54
Intercept:	0,921	Peak 3: 0,000	0,000
Result quality :	Good		

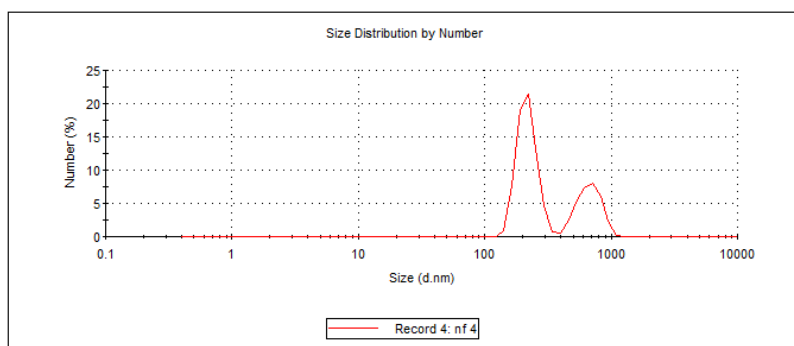


Figure S34. The size distribution of metal-organic aggregates in solution of catalytic system based on **6b**.

	Diam. (nm)	% Number	Width (nm)
Z-Average (d.nm):	1247	100,0	158,3
Pdl:	0,325	0,0	0,000
Intercept:	0,915	Peak 3: 0,000	0,000
Result quality :	Good		

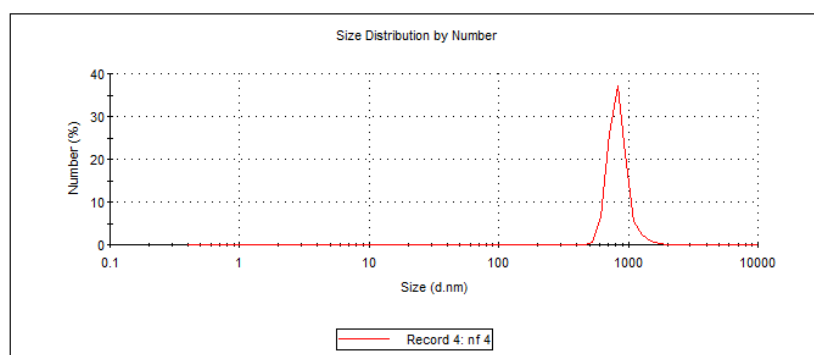


Figure S35. The size distribution of metal-organic aggregates in solution of catalytic system based on **7b**.

	Diam. (nm)	% Number	Width (nm)
Z-Average (d.nm): 818,7	Peak 1: 1144	2,1	230,7
Pdl: 0,447	Peak 2: 303,6	97,9	49,11
Intercept: 0,907	Peak 3: 0,000	0,0	0,000

Result quality : Refer to quality report

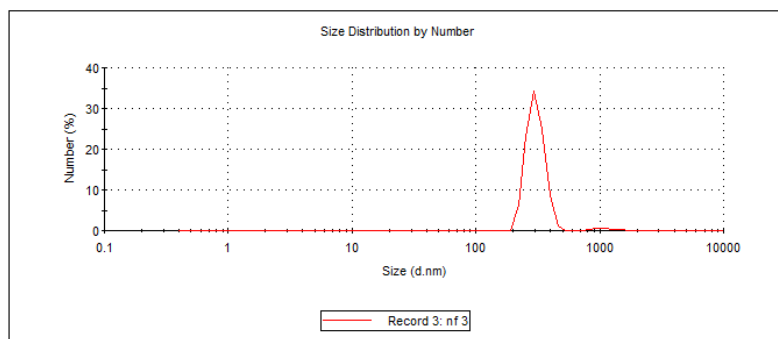


Figure S36. The size distribution of metal-organic aggregates in solution of catalytic system based on **8b**.

	Diam. (nm)	% Number	Width (nm)
Z-Average (d.nm): 1535	Peak 1: 1096	5,9	322,3
Pdl: 0,456	Peak 2: 238,0	94,1	32,65
Intercept: 0,907	Peak 3: 0,000	0,0	0,000

Result quality : Good

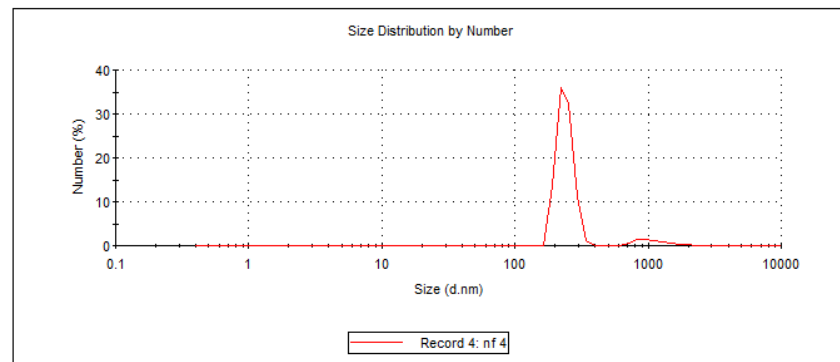


Figure S37. The size distribution of metal-organic aggregates in solution of catalytic system based on **9b**.